AD_____

Award Number: W81XWH-05-1-0013

TITLE: Temporal and Spatial Dynamics of Androgen Receptor Conformation and Interactions in Prostate Cancer Cells

PRINCIPAL INVESTIGATOR: Fred Schaufele, Ph.D.

CONTRACTING ORGANIZATION: University of California San Francisco
San Francisco, CA, 94143

REPORT DATE: November 2007

TYPE OF REPORT: Final

PREPARED FOR: U.S. Army Medical Research and Materiel Command
Fort Detrick, Maryland 21702-5012

DISTRIBUTION STATEMENT: Approved for Public Release;
Distribution Unlimited

REPORT DOCUMENTATION PAGE

Form Approved
OMB No. 0704-0188

1. REPORT DATE *(DD-MM-YYYY)*	**2. REPORT TYPE**	**3. DATES COVERED** *(From - To)*
01-11-2007	Final	15 OCT 2004 - 14 OCT 2007

4. TITLE AND SUBTITLE

Temporal and Spatial Dynamics of Androgen Receptor Conformation and Interactions in Prostate Cancer Cells

5a. CONTRACT NUMBER

5b. GRANT NUMBER
W81XWH-05-1-0013

5c. PROGRAM ELEMENT NUMBER

6. AUTHOR(S)
Fred Schaufele, PhD

E-Mail: freds@diabetes.ucsf.edu

5d. PROJECT NUMBER

5e. TASK NUMBER

5f. WORK UNIT NUMBER

7. PERFORMING ORGANIZATION NAME(S) AND ADDRESS(ES)

University of California San Francisco
San Francisco, CA, 94143

8. PERFORMING ORGANIZATION REPORT NUMBER

9. SPONSORING / MONITORING AGENCY NAME(S) AND ADDRESS(ES)
U.S. Army Medical Research and Materiel Command
Fort Detrick, Maryland 21702-5012

10. SPONSOR/MONITOR'S ACRONYM(S)

11. SPONSOR/MONITOR'S REPORT NUMBER(S)

12. DISTRIBUTION / AVAILABILITY STATEMENT
Approved for Public Release; Distribution Unlimited

13. SUPPLEMENTARY NOTES

14. ABSTRACT
Our long-term goal is to correlate the undesired escape from androgen deprivation therapy with specific molecular events in Androgen Receptor signaling in order to determine the best molecular targets for prostate cancer treatment. Studies supported by this grant indicate that the failure of tumors to respond to anti-androgen therapy corresponded best with an increased nuclear transport of AR. However, an intramolecular fold and AR dimerization, both activated abnormally by heterologous hormones (estrogen and progestin) and measured by fluorescence resonance energy transfer of CFP and YFP-tagged ARs), also was linked to four different AR mutants associated with treatment-refractory prostate proliferation. High throughput methods were developed to measure AR folding, dimerization and nuclear transport. These methods will facilitate the future identification of new drugs that block AR folding, dimerization and nuclear transport and that may prove useful in treatment-refractory therapy.

15. SUBJECT TERMS
Prostate Cancer, Resistance to Therapy, Anti-Androgen, Androgen Receptor, Structure

16. SECURITY CLASSIFICATION OF:			**17. LIMITATION OF ABSTRACT**	**18. NUMBER OF PAGES**	**19a. NAME OF RESPONSIBLE PERSON**
					USAMRMC
a. REPORT	**b. ABSTRACT**	**c. THIS PAGE**			**19b. TELEPHONE NUMBER** *(include area code)*
U	U	U	UU	27	

Standard Form 298 (Rev. 8-98)
Prescribed by ANSI Std. Z39.18

Table of Contents

Introduction

In 2003, 220,000 American men were diagnosed with prostate cancer (1), which represented 33% of male cancer cases. Most prostate tumors are dependent upon androgens for survival and growth. As such, the Androgen Receptor (AR) is a primary target for intervention. Treatment options that target AR include pharmacologic interventions that lower androgen synthesis, often in conjunction with AR-binding drugs that compete with androgens to block AR response activated by residual androgens (2, 3).

An unfortunate, but common, outcome of androgen deprivation treatment is the outgrowth of tumor cells adapted to grow in response to low androgen levels (4-9). Tumor adaptation has many origins, often directed at AR. For instance overexpression of AR (10-14), or altered AR modification (14-17), increase the likelihood that AR will bind an androgen at the low androgen levels present during deprivation therapy. Resistance to androgen deprivation therapy also may result from androgen-independent transport of AR to the cell nucleus (11, 18, 19), or altered levels of AR co-activators that interact with the nuclear, androgen-bound AR (10, 20, 21). Some AR mutations even allow AR antagonists to bind in a fashion that activates the AR, leading to tumor growth (4-9). For these patients, anti-androgen withdrawal provides temporary improvement (5, 22). Thus, modifications of AR, and of the cell environment regulating AR, are the primary causes of prostate cancer treatment failure.

Since tumor-specific AR mutations, modifications and alteration in co-factor balance lead to treatment failure, understanding treatment failure and improving therapy will depend on measuring androgen and anti-androgen effects on AR in tumor cell environments. This was not possible until we developed highly innovative techniques that quantify, directly in living cells, Angstrom-level, androgen-induced changes in protein structure and interactions as the amount of energy transferred between fluorescent tags attached to the protein (23-27). We have adapted these techniques to study the effects of androgens and anti-androgens on specific structural and molecular events in the AR (28). Our goal is to associate an AR structure or molecular event with prostate tumor cell growth and with resistance to hormone deprivation therapy. If realized, this would identify a suitable target for improved long-term therapies for prostate tumors and possibly identify new drugs less prone to treatment failure.

Body

Approved Statement of Work:

Task 1
Conformation, dimerization, nuclear transport and activity of flutamide-resistant, AR mutants (completion of baseline work in AR-negative HeLa cells)
22 months effort. Months 1-24.

Task 2
Conformation, dimerization, nuclear transport and activity of AR in different prostate cancer cell environments.
28 months effort. Months 12-36.

Task 3
AF-2 interaction with FQNLF in the DHT-induced re-positioning of AF-1 towards the LBD.
15 months effort. Months 6-30.

The Tasks are summarized in Fig. 1. All Tasks were completed within the project time frame with results of the past year currently being finalized for publication. We also developed new understandings of AR action and technical capabilities that were unanticipated at the project onset.

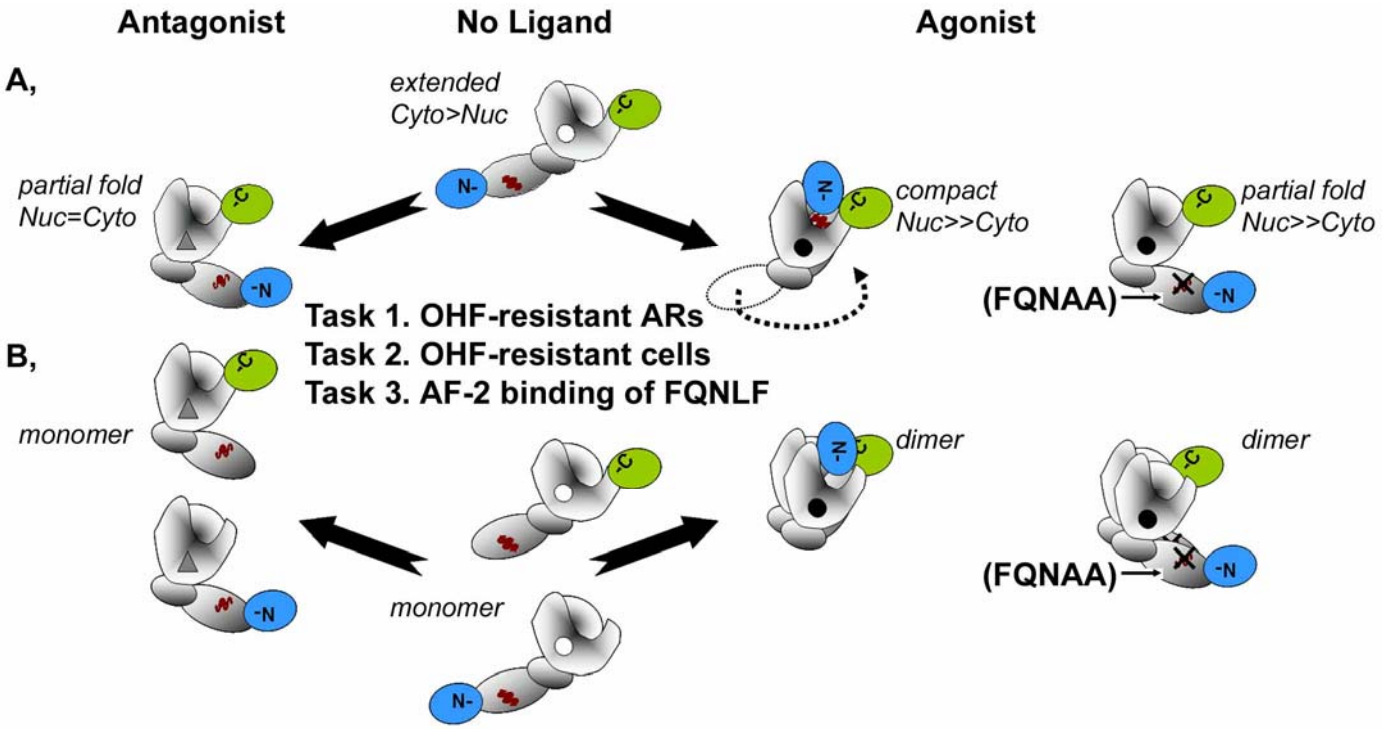

Fig. 1. Fluorescence Resonance Energy Transfer analysis of the effects of androgens and anti-androgens on **A,** intramolecular folding and **B,** dimerization of the Androgen Receptor. **The goal is to define whether intramolecular folding, dimerization or cytoplasm-to-nucleus transport is associated with the blockage of prostate tumor cell proliferation and if the failure to respond to anti-androgen therapy is associated with the reacquisition of any of these molecular events.**

Task 1 Final Report.

Task 1: Conformation, dimerization, nuclear transport and activity of flutamide-resistant, AR mutants (completion of baseline work in AR-negative HeLa cells)

Outcome: *The intramolecular folding of AR (CFP-AR-YFP FRET), AR dimerization (CFP-AR/AR-YFP FRET) and the nuclear transport of the AR all correlated with the development of treatment failure for four different AR mutations. A subset of the mutations and ligands studied were published in PNAS. We currently are finishing the figures to submit (most likely to Cancer Research) the comprehensive analysis reported below.*

1a. Construct T877A, T877S, H874Y and V715M mutants in the CFP-AR and AR-YFP expression vectors. Construct the V715M mutant in the CFP-AR-YFP expression vector.
Completed

- The constructs were completed albeit with some problems commented on in the Year 02 report.
- The effects of the mutations on AR structure, (all Tasks) were conducted by analyzing energy transfer within an Androgen Receptor fused on opposite ends with CFP and YFP (see Fig. 1A). In order to investigate the effects of those same mutations on AR dimerization (all Tasks), we analyzed energy transfer between different ARs, one fused with CFP and the other with YFP (see Fig. 1B). Nuclear localization studies were completed using the image data collected for the FRET studies.

1b. Determine rapid (1-20 mins) and long-term (0.5, 1, 2 and 5 hrs) changes in dimerization of wild-type, T877A, T877S, H874Y and V715M CFP-AR and AR-YFP upon treatment with 10^{-9}M DHT, 10^{-7}M OHF, 10^{-7}M Cas, 10^{-7}M E2 or 10^{-7}M Prog.
Completed.

• We studied dimerization of the wild-type CFP-AR and AR-YFP in HeLa cells (Fig. 2A). The results of those studies conducted are summarized below. Only the initial characterization of this assay was published in our *Proceedings of the National Academy of Sciences USA* manuscript (28). Those initial studies showed that dimerization occurred specifically in the nucleus of the cell starting around five minutes following the addition of DHT (Fig. 2B, closed boxes). Dimer acquisition in the cytoplasm was much slower (open boxes), but reaches the level found in the nucleus within one hour of DHT addition (not shown). Note that DHT also initiated transport of the AR from the cytoplasm to the nucleus (Task 1d). The FRET measurements shown in all figures depict the extent of dimerization per unit of AR, which is a measurement not affected by the total amount of AR in the nucleus and cytoplasm as it changes with nuclear import.

• Fig 2C shows that, for the interaction between two fluorophore-tagged proteins (CFP-AR and AR-YFP), the amount of energy transfer (FRET/Donor) increases to a saturation point as the amount of acceptor-labeled factor (AR-YFP) in the cell is increased relative to the amount of donor-labeled factor (CFP-AR) (23-28). In the presence of DHT, the data points of this graph fit very well to the mathematical binding curve that describes a biochemical interaction between two proteins (Fig. 2C, closed boxes). There is no energy transfer and no fit to the curve if the cells are not treated with ligand or are treated with OHF (Fig. 2C). The addition of excess OHF blocked the DHT-induction of AR dimerization measured by FRET in a dose-dependent fashion (28) (not shown). Thus, OHF, which blocks androgen-dependent proliferation of prostate cancer cells, also blocks androgen-dependent AR dimerization.

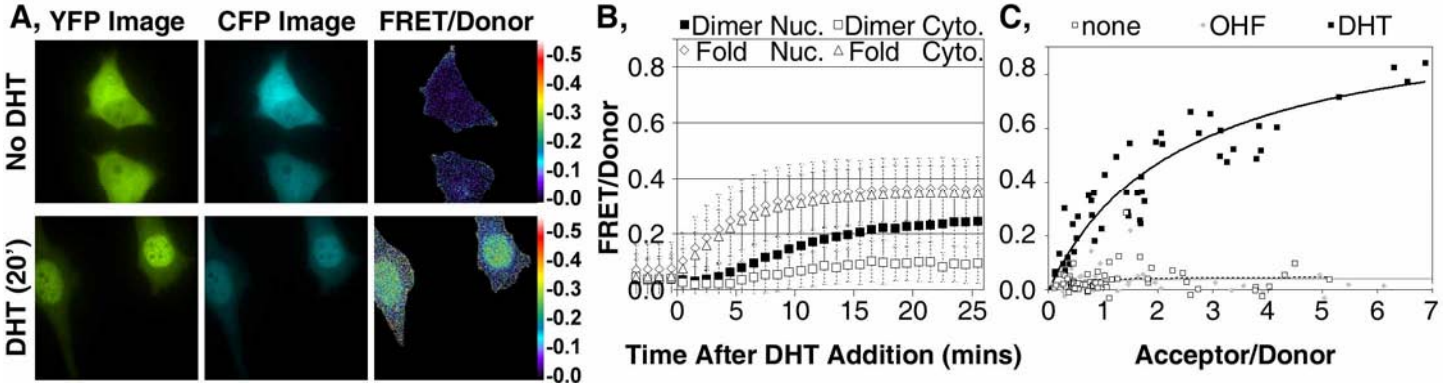

Fig. 2. Energy Transfer within and between wild-type CFP-AR and wild-type AR-YFP in HeLa cells. **A,** Representative images of single cells captured when incubated for 20 minutes with DHT (DHT 20') or 20 minutes with vehicle (No DHT). The FRET/Donor image is calculated from the YFP, CFP and FRET images according to our previously published methods (23-28). The amounts of energy transfer per unit AR amount range from low (0) to high (0.5) in the FRET/Donor image (color bars). **B,** FRET/Donor values in the nucleus or cytoplasm of the cell averaged from multiple different cells (mean +/- s.d.) at the indicated time points following DHT addition. Dimer, energy transfer amounts between CFP-AR and AR-YFP (Task 1b). Fold, energy transfer between CFP and YFP within a single AR (Task 1c, CFP-AR-YFP). **C,** Kinetics of interaction between CFP-AR and AR-YFP. Interaction in the presence of DHT follows a curve indicative of interaction between two factors (Law of Mass Action). OHF does not promote interaction between CFP-AR and AR-YFP (28).

• One goal of the studies was to establish whether AR mutants (that are associated with a failure to respond to anti-androgen therapy) resulted in any abnormal dimer formation in response to anti-androgens, or in response to any other ligand present. Four such treatment-refractory AR mutants were analyzed for their effects on dimerization of AR-CFP and AR-YFP (Fig. 3). Compared to wild-type AR (Fig. 3A), the dimerization of all four AR mutants (Figs. 3B-E) show the same abnormal, elevated dimerization in the presence of the anti-androgen hydroxyflutamide (OHF, lime line) and the heterologous ligands estradiol and progesterone (blue lines). Interestingly, the anti-androgen Casodex did not elicit these responses (orange line). At the time of filing this report, these studies have been completed a total of three times. Thee averaged data will be included with our other remaining studies (described in this report) in a manuscript that we anticipate to submit to *Cancer Research*.

• *Conclusions of Task 1b:*
The anti-androgens, hydroxyflutamide and Casodex, did not promote dimerization of AR. However, abnormal dimerization in the presence of hydroxyflutamide or two heterologous ligands was observed for AR mutations associated with treatment failure. This may be an important factor in the mechanism by which some tumors escape anti-androgen blockade of prostate tumor growth.

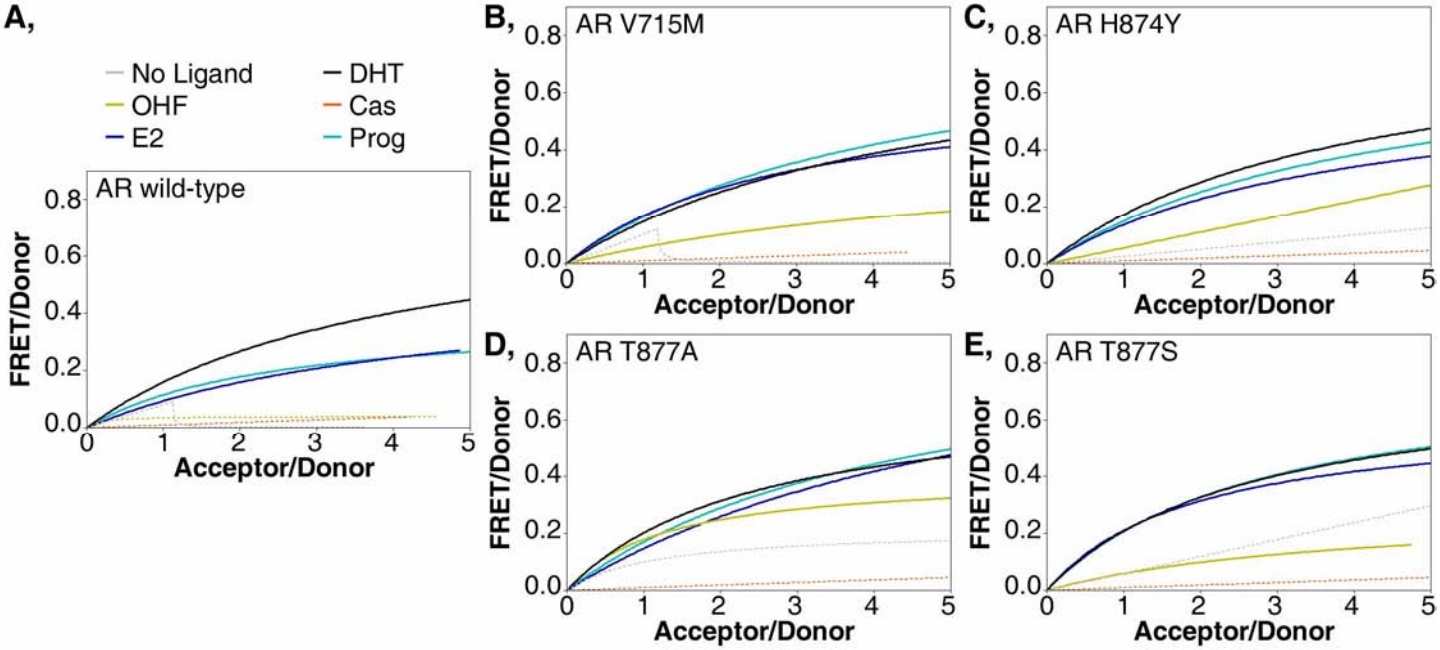

Fig. 3. A, Dimerization of AR-CFP and AR-YFP in HeLa cells treated for one hour with dihydrotestosterone (DHT), hydroxyflutamide (OHF), casodex (Cas), estradiol (E2) or progesterone (Prog). Curves in which the data points fit well to a bimolecular interaction profile (R^2>0.7) are shown as solid line and indicate dimerization in response to the ligand. Curves not fitting well are indicated as dotted lines and indicate poor dimerization. **B-E,** Four different hormone refractory AR mutants all allow enhanced (compared to wild-type AR) in response to OHF, E2 and Prog. Dimerization in response to E2 and Prog shifts to the levels observed with the wild-type AR incubated with DHT.

1c. Determine rapid (1-20 mins) and long-term (0.5, 1, 2 and 5 hrs) changes in intramolecular folding of wild-type, T877A, T877S, H874Y and V715M CFP-AR-YFP upon treatment with 10^{-9}M DHT, 10^{-7}M OHF, 10^{-7}M Cas, 10^{-7}M E2 or 10^{-7}M Prog.
Completed

• Time course studies with the wild-type CFP-AR-YFP established that the acquisition of energy transfer following DHT addition was very rapid (28), occurred with equal efficacy in the cytoplasm and in the nucleus (Fig. 4A) and was essentially complete by 1 hour (Fig. 4B). The energy transfer of the CFP-AR-YFP sensor resulted from the induction, by DHT, of both an intramolecular fold within the AR and of a dimerization between ARs (Task 1b) that bring the CFP and YFP into close enough proximity to permit energy transfer. Detailed time course analysis of CFP-AR-YFP FRET compared to the dimer FRET between CFP-AR/AR-YFP (Fig. 2B) and between CFP-AR-CFP/YFP-AR-YFP (data not shown) showed that the energy transfer within CFP-AR-YFP preceded the energy transfer between the ARs (28)(Fig. 2B), i.e. the rapid intramolecular fold is followed 5 minutes later, on average, by dimerization in the cell nucleus. Cytoplasmic dimerization occurs much later.
• The analysis of CFP-AR-YFP folding in the T877A, T877S and H874Y hormone-refractory prostate cancer mutants was published in the *Proceedings of the National Academy of Sciences USA* (28). The manuscript is provided as an Appendix to this report. That data, together with more recent work on a fourth hormone refractory prostate cancer mutant (V715M) and the response to Casodex, is summarized in Fig. 5 and discussed below.

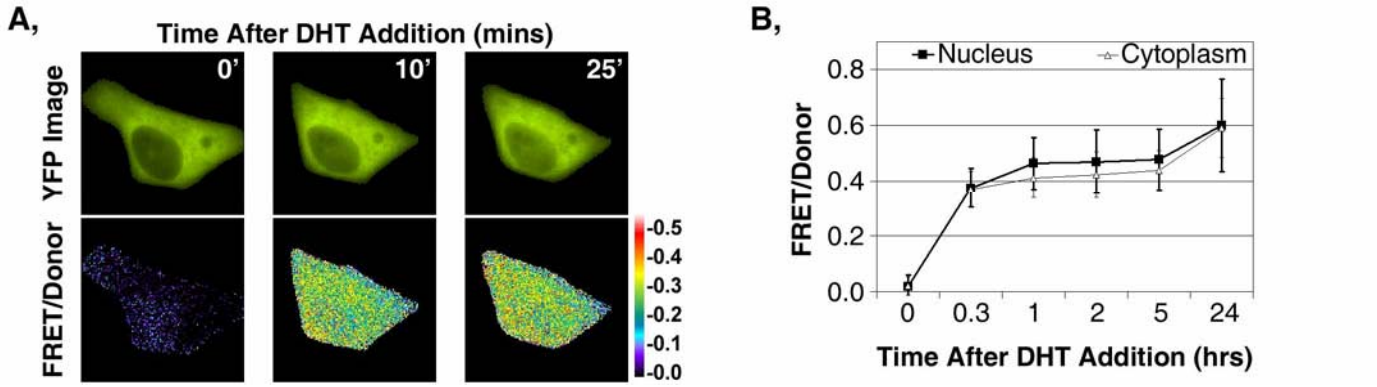

Fig. 4. Energy Transfer within and between wild-type CFP-AR-YFP. **A,** Representative images of the time course of a single cell; images were capture at 1 minute intervals before (0') or after DHT addition. YFP image, fluorescence that marks the cellular location of CFP-AR-YFP. FRET/Donor, positions of energy transfer ranging from low (0) to high (0.5, see scale bar) for the corresponding cell. **B,** FRET/Donor values in the nucleus or cytoplasm averaged from multiple different cells (mean +/- s.d.) at the indicated time points following DHT addition. By the 24 hour time period, very few cells have much cytoplasmic AR remaining and the FRET/Donor values indicated are only from the cells that transport AR poorly.

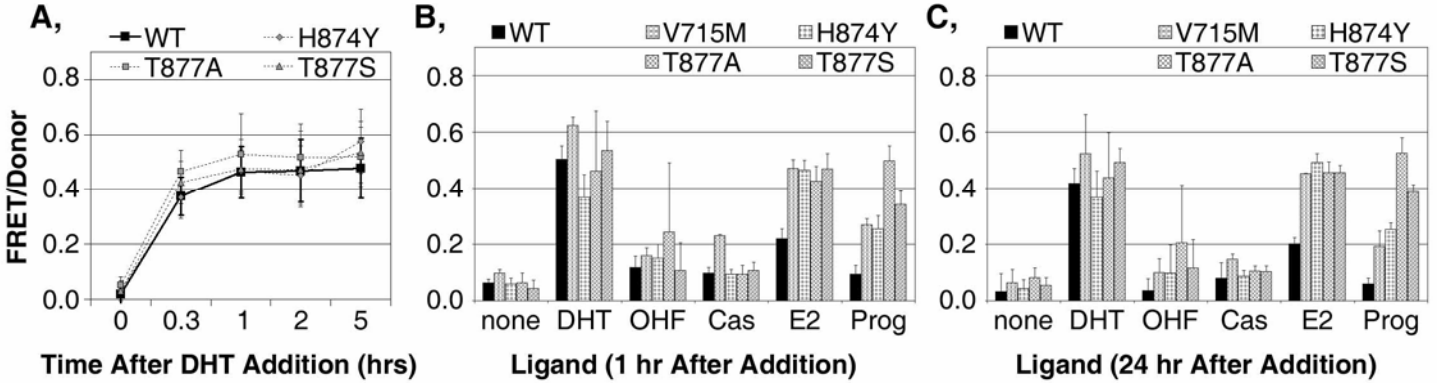

Fig. 5. The effects of point mutations in AR associated with hormone-refractory prostate cancer on Energy Transfer by CFP-AR-YFP. **A,** The temporal and quantitative responses of the H874, T877A and T877S mutants to DHT are identical to wild-type AR. **B, C,** The V715M, H874Y, T877A and T877S mutants show improved intramolecular folding, compared to wild-type AR (black bars), in response to estradiol. The mutants also show improved responses to progesterone, the extent of which varies with the ligand. More modest activation of folding was observed with hydroxyflutamide (T877A-specific) and Casodex (V715M-specific).

• Time course studies on CFP-AR-YFP FRET for the T877A, T877S and H874Y prostate cancer mutants established that their intramolecular folding/dimerization response to DHT is temporally identical to that of the wild-type AR (Fig. 5A). For all data shown in Fig. 5, only the folding/ dimerization response in the nucleus is shown; the response measured in the cytoplasm was not statistically different than that in the nucleus for all mutants at most collection points.

• Four different mutations in AR that are associated with anti-androgen treatment failure showed enhanced energy transfer (compared to wild-type AR) in the presence of various ligands (Figs. 4B, C). Interestingly, the V715M mutant responded well to the newer generation anti-androgen Casodex whereas the T877A mutant responded more to hydroxyflutamide. Depending on the extent to which the CFP-AR-YFP FRET acts as a marker of prostate tumor cell response, this may suggest that Casodex and OHF may be complementary in some instances of treatment resistance. Note that, for all mutants, the responses to estradiol and progesterone are much more striking that to the anti-androgens.

• *Conclusions of Task 1c:*

The androgen dihydrotestosterone promoted an intramolecular fold in the AR receptor that preceded nuclear transport. Pharmacologic levels of the heterologous ligands estradiol and progesterone also promote the intramolecular fold. AR mutants found in some patients with resistance to androgen deprivation therapy display a much stronger ability to fold in response to the anti-androgens Casodex

and hydroxyflutamide and to the heterologous ligands (estradiol, progesterone). As suggested by others, responses to the heterologous ligands may be the more clinically pertinent component in the acquisition of anti-androgen resistance.

1d. Determine rapid (1-20 mins) and long-term (0.5, 1, 2 and 5 hrs) changes in nuclear transport of wild-type, T877A, T877S, H874Y and V715M CFP-AR-YFP upon treatment with 10^{-9}M DHT, 10^{-7}M OHF, 10^{-7}M Cas, 10^{-7}M E2 or 10^{-7}M Prog.
Completed.

- The images used to collect the FRET data also were used to concurrently track the relative amounts of the AR in the nucleus and in the cytoplasm. In the absence of any ligand, the concentration of wild-type CFP-AR-YFP in the nucleus is quantified as half that in the cell cytoplasm (Fig. 6A, see representative image in Fig. 4). For all quantitative analysis of nucleus/cytoplasmic partitioning, the amounts of YFP fluorescence (selectively excite YFP/collect YFP only emissions) are used since this value is unaffected by energy transfer. The values shown represent the amounts of AR fluorescence per unit area, representative of AR concentration, not the total amounts of AR corrected for the relative amounts of nuclear and cytoplasmic volume. The total amounts are more difficult to rapidly determine and would require complete three-dimensional reconstruction of the volume of each cell.
- A progressive increase in the amount of wild-type AR in the nucleus follows the addition of DHT. By 24 hours following DHT addition, almost all AR fluorescence is nuclear (on average 11 times that measured in the cytoplasm). However, the amount of wild-type AR transported into the cell nucleus is dramatically less for the anti-androgens OHF (0.72 +/- 0.16 at 24 hours) and Casodex (1.13 +/- 0.50). Nevertheless, this is significantly more than the 0.46 +/- 0.22 amounts quantified in the absence of any ligand. This demonstrates that both OHF and Casodex promote nuclear transport of AR, albeit much less effectively than does wild-type AR.
- The defective nuclear transport of AR in response to OHF and Casodex may represent a mechanism that is circumvented upon the development of treatment failure. The four AR mutations associated with treatment-unresponsive prostate cancer therefore were examined for their effects on nuclear transport. The nucleus/cytoplasmic partitioning of the H874Y and T877S mutants are not significantly different than the wild-type AR in the absence of any ligand (Fig. 6B, none). By contrast, the nuclear concentration of the T877A and V715M mutants are significantly elevated in the absence of ligand. Most importantly, all four mutants show elevated transport compared to wild-type AR in response to the antagonists and to the heterologous ligands (Figs. 6B, C).

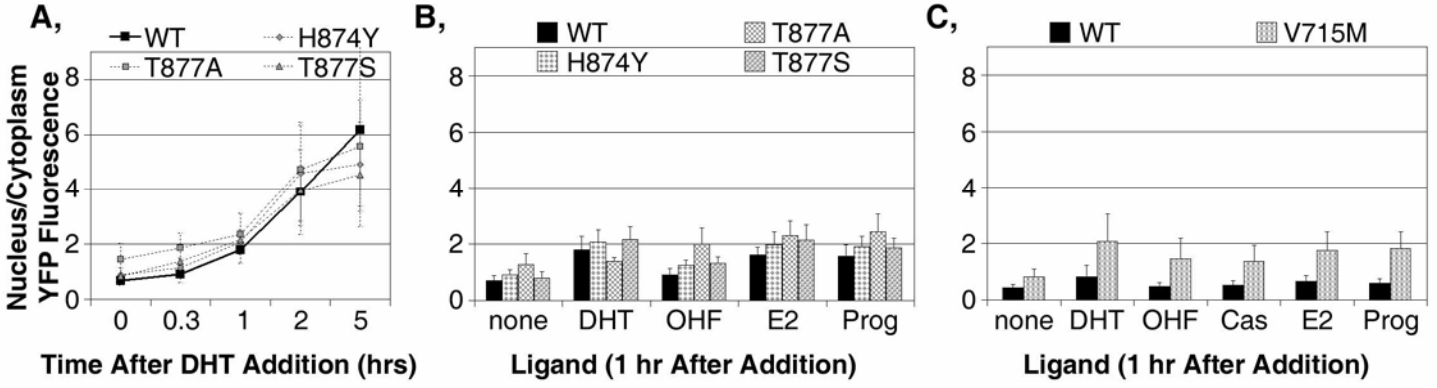

Fig. 6. The effects of point mutations in AR associated with hormone-refractory prostate cancer on the transport of CFP-AR-YFP from the cytoplasm to the nucleus. **A,** There is a statistically significant elevated amount of the T877A mutant in the nucleus in the absence of ligand. Otherwise, the responses of the H874, T877A and T877S mutants to DHT are similar to wild-type AR. **B,** The H874, T877A and T877S show improved responses to heterologous ligand (hydroxyflutamide, estradiol and progesterone) that may be associated with the ability of tumors containing those mutants to grow in response to those ligands (10^{-6}M; responses were less with 10^{-7}M ligand). The response of the T877A mutant to OHF is particularly strong. **C,** A further hormone refractory prostate cancer mutant, V715M, displays a strong, statistically significant enhancement in cytoplasm to nuclear transport in the absence of ligand and in the response to 10^{-7}M of all heterologous ligands (10^{-6}M for Casodex). All data presented as the mean +/- s.d.

• *Conclusions of Task 1d:*
AR mutants found in some patients with resistance to androgen deprivation therapy are more readily transported into the cell nucleus than is the wild-type AR. There are some mutant-specific differences in the basal level this improved transport.

1e. Determine transcriptional activation of androgen-sensitive reporters by unfused AR and wild-type, T877A, T877S, H874Y and V715M CFP-AR, AR-YFP and CFP-AR-YFP fusions upon treatment with 10^{-7}M OHF, 10^{-7}M Cas, 10^{-7}M E2 or 10^{-7}M Prog.
Completed.

•The work was were published in the *Proceedings of the National Academy of Sciences USA* (28). The manuscript is provided as an Appendix to this report. That analysis showed that the mutant CFP-AR-YFP fusion proteins all activated a reporter in response to OHF whereas transcriptional activity of the wild-type AR was inhibited. Furthermore, all mutants showed enhanced transcriptional activity in response to pharmacologic levels of estradiol and progesterone compared to wild-type AR.
•As mentioned in the Year 02 report, we had difficulties with the singly-labeled AR-YFP and CFP-AR expression vectors that were resolved only recently. Therefore the mutants were not analyzed for transcriptional activity in these vector backgrounds. Given that the wild-type AR-YFP and CFP-AR behave functionally identical to the CFP-AR-YFP vectors in reporter activation assays (our PNAS paper, 28), we have every reason to suspect that the hormone refractory mutants would behave the same in the AR-YFP and CFP-AR background as reported in the CFP-AR-YFP background (our PNAS paper, 28).

• *Conclusions of Task 1e:*
The CFP-AR-YFP fusion proteins retain the previously described transcriptional responses described for the known AR mutations associated with failure to respond to anti-androgen therapy. This is an important control for establishing the relative abilities of the transcriptional reporter and of the FRET analyses and nuclear transport analyses to predict the hormone refractory phenotype. The effects on transcriptional response measured by the reporter assays are far downstream of the immediate effects of the androgens, anti-androgens and heterologous ligands on the AR, measured by the FRET and transport assays.

Task 2 Progress

Task 2: Conformation, dimerization, nuclear transport and activity of AR in different prostate cancer cell environments.
Completed.

• The rationale for conducting these studies was the hypothesis that hormone-insensitive cell lines (such as LNCaP-C4-2) would display activated intramolecular CFP-AR-YFP FRET, dimer CFP-AR/AR-YFP FRET or enhanced nuclear transport of AR in the absence of ligand. Alternatively, the hypothesis was that either or both FRET responses would be activated at lower levels of DHT in these hormone-insensitive cell lines.

Outcome to date: *We established an enhanced basal nuclear transport of the AR in the LNCaP-C4-2 cells, which correlated with their ability to grow in response to no ligand. By contrast, no correlation was observed of growth with the intramolecular folding of AR measured by CFP-AR-YFP FRET or with dimerization of AR-CFP with AR-YFP.*

2a. Construction of expression vectors for AR-fusion proteins
Completed.

• The expression constructs for the fusion proteins, and mutants thereof, were identical to those already constructed for Aim 1a.

2b. Determine, in androgen-sensitive LNCaP, LNCaP-C4-2 and CWR-R1 prostate cancer cells and in AR-null HeLa cells, the rapid (1-20 mins) and long-term (0.5, 1, 2 and 5 hrs) changes upon treatment with seven different concentrations of DHT ranging from 10^{-14}M to 10^{-8}M, four different concentration of OHF ranging from 10^{-10}M to 10^{-7}M and 10^{-7}M Cas of:
i. dimerization of wild-type, T877A, and H874Y CFP-AR and AR-YFP
ii. conformation of wild-type, T877A, and H874Y CFP-AR-YFP
iii. nuclear transport of wild-type, T877A, and H874Y CFP-AR, AR-YFP and CFP-AR-YFP

• Perhaps the most difficult component of this Task was defining methods for attaining efficient introduction of the vectors to express the AR fusions with CFP and YFP into the prostate cancer cell lines. Multiple transfection methods were employed. Comparison between the cell lines requires that all conditions, including transfection type and AR expression levels following transfection, are similar between the cell lines studied. That is necessary because an experimental difference could introduce variables into the results that would affect our ability to ascribe any observed difference in the results to actual differences in the cell types. Overall, we determined that the 'Effectine' transfection reagent worked best for both the LNCaP cell line and its anti-androgen-resistant (enhanced DHT-sensitive) derivative, LNCaP-C4-2. We were not able to successfully grow the CWR-R1 hormone-sensitive line. All studies therefore were completed on the LNCaP and LNCaP-C4-2 cells.

i. dimerization of wild-type, T877A, and H874Y CFP-AR and AR-YFP
Mostly Completed.

• The rationale for conducting the studies with the T877A and H874Y mutants was that the endogenous ARs present in the LNCaP-C4-2 and CWR-R1 cells contained those specific mutations, respectively. Since we were able only to obtain growth of the LNCaP-C4-2 cells, we limited our studies to that mutant in those cells. We observed no difference in DHT dose response for the dimerization of either wild-type or T877A AR in either cell-type. We then had some difficulties culturing the LNCaP cells but anticipate we will have these studies completed by the end of 2007 to include in the manuscript we anticipate to submit soon to *Cancer Research*.

ii. conformation of wild-type, T877A, and H874Y CFP-AR-YFP
Completed.

• We completed the DHT dose response curves for energy transfer using the CFP-AR-YFP vectors in the LNCaP and LNCaP-C4-2 cell lines. There was no statistically significant elevation in the amount of CFP-AR-YFP FRET in the LNCaP-C4-2 cell line in the absence of ligand (Fig. 7A), which also was not different that that observed in the AR-null HeLa cells (compare with Fig. 5, HeLa cells). The DHT dose response curve for the acquisition of CFP-AR-YFP FRET (wild-type AR) also was exactly the same in LNCaP and LNCaP-C4-2 cells (Fig. 7A). Measurements were made at 30 minutes after the addition of DHT, a time after which the acquisition of FRET is complete. The requirement for 'normal' concentrations of androgen to allow the CFP-AR-YFP to fold in the androgen-independent LNCaP-C4-2 cells indicates that this intramolecular fold is <u>not</u> a general marker of the changes in the AR that permit those cells to proliferate in the absence of androgen. This contrasts with the results observed in Task 1, in which the intramolecular folding correlated with the AR mutants associated with androgen-independence.

• It remains possible that the androgen-independent growth of the LNCaP-C4-2 cells may rely on an androgen-independent acquisition of folding by the endogenous AR, which is the T877A mutant of AR. We anticipate completion of the comparison of the wild-type and T877A AR before the end of 2007. That data would be necessary before we can formally conclude that the intramolecular fold does not act as a marker for the acquisition of androgen-independent cell growth in this particular hormone-insensitive cell line. Regardless of outcome, the data will be included in the manuscript we anticipate to submit soon to *Cancer Research*.

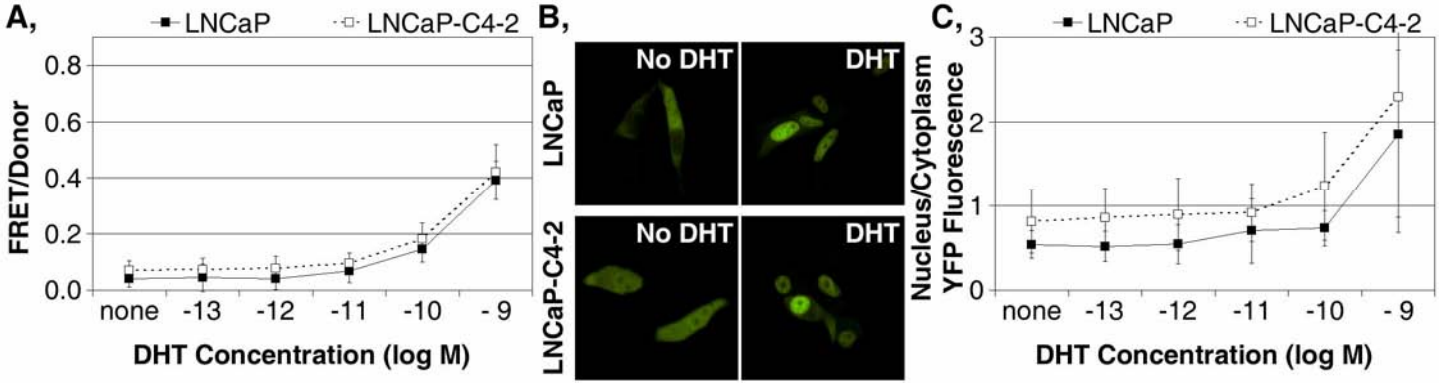

Fig. 7. DHT dose response for CFP-AR-YFP intramolecular FRET and nuclear transport in LNCaP prostate cancer-derived cells and in the LNCaP-C4-2 derivate that grows in the absence of added androgens. **A,** No statistically significant difference in CFP-AR-YFP FRET detected between LNCaP and LNCaP-C4-2 cells. **B,** In the absence of any added DHT (none), CFP-AR-YFP is markedly more nuclear in LNCaP-C4-2 cells than in LNCaP cells. Both cell lines respond rapidly when treated with 10^{-9}M DHT for 30 minutes. YFP images are shown. **C,** The DHT dose response profile is identical for LNCaP and LNCaP-C4-2 cells. All quantified data presented as the mean +/- s.d.

iii. nuclear transport of wild-type, T877A, and H874Y CFP-AR, AR-YFP and CFP-AR-YFP
Completed.

• We completed the DHT dose response curves for nuclear transport using the CFP-AR-YFP vectors in the LNCaP and LNCaP-C4-2 cell lines. In the absence of ligand, the amount of CFP-AR-YFP in the cell nucleus was significantly elevated in the LNCaP-C4-2 cell line (Fig. 7B) compared to the LNCaP cells (Fig. 7B) and to the AR-null HeLa cells (Fig. 6). Quantitative data collected and averaged from multiple cells (Fig. 7C) confirm that conclusion. Interestingly, however, the dependence of AR transport in the androgen-insensitive LNCaP-C4-2 cells still follows the same dose response to DHT observed for LNCaP (Fig. 7C) and HeLa (not shown) cells. This would suggest that any association of enhanced nuclear transport with the acquired androgen-insensitivity of the LNCaP-C4-2 model would have to originate from true androgen-independence rather than from a heightened response to lower levels of androgen. Indeed, a recent manuscript demonstrated the same enhanced nuclear localization in LNCaP-C4-2 cells the absence of ligand that is retained even if the ligand binding pocket of the AR is disrupted by mutation (29).
• Visual inspection of large numbers of images with have collected to date clearly shows no difference in the nuclear transport and dose response properties of the T877A and wild-type AR-YFP in LNCaP-C4-2 and LNCaP cells. Firm conclusions await the final quantification of those images. We also will complete those comparisons with the CFP-AR-YFP constructs (see prior section). Formal characterization is unlikely to alter the clear conclusion apparent upon visual inspection but will be done to include in the manuscript being prepared for submission.

• *Conclusions of Task 2b:*
The ability of AR to fold or to dimerize did not correlate with the enhanced growth of the LNCaP-C4-2 cell line in the absence of androgen. However, an enhanced basal level of nuclear transport correlated very well with enhanced growth.

2c. Determine transcriptional activation of androgen-sensitive reporters by
i. endogenous AR in androgen-sensitive LNCaP, LNCaP-C4-2 and CWR-R1 prostate cancer cells.
ii. transiently expressed unfused AR and wild-type, T877A and H874Y CFP-AR, AR-YFP and CFP-AR-YFP fusions in AR-null HeLa cells.
All cells will be treated with vehicle, seven different concentrations of DHT ranging from 10^{-14}M to 10^{-8}M, four different concentration of OHF ranging from 10^{-10}M to 10^{-7}M and 10^{-7}M Cas.
Partially Completed.

- Owing to difficulties with the growth of the LNCaP cells, these studies were delayed. We anticipate that we will complete these relatively minor studies to include in the manuscript being prepared for submission to *Cancer Research*.

Task 3 Progress

Task 3: **AF-2 interaction with FQNLF in the DHT-induced re-positioning of AF-1 towards the LBD.**
Completed.

- The rationale for conducting these studies was the hypothesis that the intramolecular fold measured by CFP-AR-YFP FRET correlated with the ability of the AR H874Y, T877A, T877A and V715M mutants to grow in the presence of anti-androgens and heterologous ligands. Therefore, establishing the molecular mechanism by which the fold occurred was thought to be critical to understanding the development of treatment failure.

Outcome: *We established that the androgen-regulated intramolecular fold between the amino and carboxy terminus of the AR depended upon the 'FQNLF' motif in the amino terminus and the 'AF-2' motif in the carboxy terminus. This was the hypothesized outcome.*

3a. Construct V716R, I898T and K720A mutants in CFP-AR, AR-YFP and CFP-AR-YFP expression vectors. Obtain V716F and F27A mutants in CFP-AR, AR-YFP and CFP-AR-YFP expression vectors.
* *Completed.*

- The V716F and F27A mutants were constructed, as was a deletion of the entire five amino acids of the FQNLF motif (ΔF). As indicated in Task 3b, these mutants alone provided sufficient evidence that the FQNLF and AF-2 motifs in the amino and carboxy terminus, respectively, of the AR were required for the intramolecular AF fold. The remaining mutations therefore were not introduced. If the dimerization studies in the androgen-insensitive cell line (Task 2) suggest an involvement in hormone refractory response of the positions of the amino and carboxy termini of the AR dimer, we would then construct the V716R, I898T and K720A mutants in the CFP-AR and AR-YFP expression vectors. That would require approximately two weeks of total effort.

3b. Determine in AR-null HeLa cells the rapid (1-20 mins) and long-term (0.5, 1, 2 and 5 hrs) changes in
i. dimerization of wild-type, V716R, I898T, K720A, V716F, F27A and the V716F/F27A complementary combination in CFP-AR and AR-YFP.
ii. conformation of wild-type, V716R, I898T, K720A, V716F, F27A and the V716F/F27A complementary combination in CFP-AR-YFP.
iii. nuclear transport of wild-type, V716R, I898T, K720A, V716F, F27A and the V716F/F27A complementary combination in CFP-AR, AR-YFP and CFP-AR-YFP.
All cells treated with 10^{-8}M DHT.

i. dimerization of wild-type, V716R, I898T, K720A, V716F, F27A and the V716F/F27A complementary combination in CFP-AR and AR-YFP.
Completed

• Initially, we conducted a FRET analysis of the effect of completely eliminating the FQNLF motif on dimerization (Fig. 8A). As indicated in Task 1b (Fig. 2), FRET analysis of an intermolecular interaction relies on establishing the amounts of energy transfer over a range of acceptor amounts, relative to donor. From that, we can extrapolate the amount of acceptor required to saturate binding. This demonstrated that the DHT-dependent interaction of CFP-AR∆F with AR∆F-YFP required the same amount of acceptor (i.e. had the same affinity) as wild-type CFP-AR with AR-YFP in living HeLa cells. That finding, reported in our published manuscript (28)(attached as an appendix) demonstrated that the FQNLF motif was not required for dimerization. Although the wild-type and ∆F ARs dimerized with equal affinity, note that the final positions of the amino and carboxy termini were different in these two complexes, as shown by the different levels of FRET at saturating amounts of acceptor. For more details on this analysis, the reader is referred to our manuscript (28) attached in the appendix and to a recently published manuscript from our laboratory describing the analyses for another factor (30).
• The initial studies with the ∆F mutant showed that the formation of the AR dimer did not depend upon the FQNLF motif. Therefore, the analysis of the effects of the V716R, I898T, K720A, V716F, F27A and the V716F/F27A mutations on AR dimerization assumed a lower priority. As we needed to troubleshoot other studies, we were unable to complete the analysis of these low priority mutants.

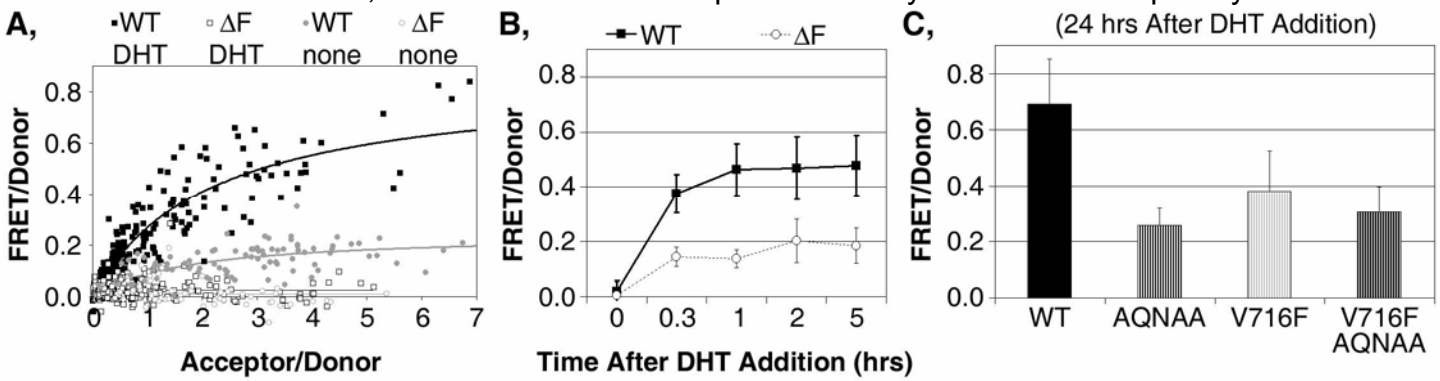

Fig. 8. The proper structure of the AR depends upon an interaction of the FQNLF motif in the AR amino terminus with the AF-2 motif in the AR carboxy terminus. **A,** Deletion of the FQNLF motif disrupts the final positions of the CFP and YFP fluorophores in the AR dimer. FRET is measured between CFP-AR and AR-YFP. The same amount of AR-YFP is required to saturate binding for the ∆F mutant, indicating no impact of the FQNLF motif on dimerization *per se*. However, the final amount of FRET is changed indicating an effect on the structure of the AR dimer. **B,** Deletion of FQNLF affects the final position of CFP and YFP in CFP-AR-YFP, but has no effect on the temporal kinetics of folding. **C,** Point mutations in FQNLF and in AF-2 (V716F) both disrupt folding of CFP-AR-YFP. All quantified data presented as the mean +/- s.d.

ii. conformation of wild-type, V716R, I898T, K720A, V716F, F27A and the V716F/F27A complementary combination in CFP-AR-YFP.
Completed.

• Initial studies of the complete deletion of the FQNLF motif in the amino terminus of AR (within the CFP-AR-YFP construct) showed that the amount of 'folding' energy transfer was decreased if the FQNLF motif was deleted (Fig. 8B). This was conceptually similar to the results obtained for the dimerization studies (Task 3bi) which showed that the FQNLF motif was responsible for positioning the amino terminus of AR in the correct location relative to the carboxy terminus.
• Even though the deletion of the FQNLF motif affected the final position of the fluorophores in CFP-AR-YFP, the temporal kinetics of folding was not different between wild-type and ∆F CFP-AR-YFP (Fig. 8B).

• Point mutations that change the FQNLF motif to AQNAA also disrupted folding of CFP-AR-YFP (Fig. 8C). A single point mutation (V716F) in AF-2, the presumed site in the AR carboxy terminus into which FQNLF binds, affected energy transfer within CFP-AR-YFP similarly to the AQNAA mutation (Fig. 8C). A V716F/AQNAA double mutation similarly reduced energy transfer. The double mutation was created on the assumption of a structural model that suggested it may be possible to regenerate the binding amino-to-carboxy terminus binding permitting an interaction of the V716F with AQNAA. The goal was to use disruption/regeneration of the interaction to firmly establish the importance of the amino-to-carboxy terminus interactions in any biologic functions. The data indicated that the amino-to-carboxy terminus interaction was not regenerated with those complementary mutations.

iii. nuclear transport of wild-type, V716R, I898T, K720A, V716F, F27A and the V716F/F27A complementary combination in CFP-AR, AR-YFP and CFP-AR-YFP.
Completed.

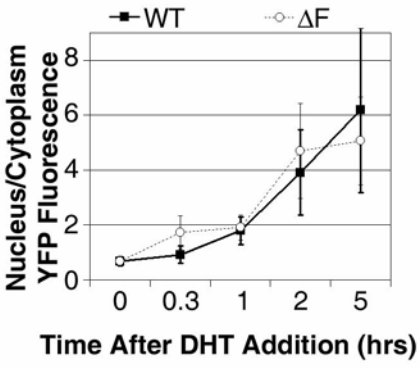

The nuclear transport data for all the mutations in Task 3bi and 3bii are present within the images collected for those studies. To date, we have conducted the analyses on the ΔF time series. That data is shown in Fig. 9. We have yet to have the time to complete the studies for the V716F, AQNAA and V716F/AQNAA studies but, visually, those mutations behaved like the ΔF mutation in that they display no overt effect on the ability of AR to be transported into the cell nucleus.

Fig. 9. Nuclear transport rates of the wild-type and ΔF CFP-AR-YFP in HeLa cells. All quantified data presented as the mean +/- s.d.

3c. Determine transcriptional activation of androgen-sensitive reporters by unfused AR and wild-type, I898T, K720A, V716F, F27A and the V716F/F27A complementary combination in CFP-AR, AR-YFP and CFP-AR-YFP following treatment of HeLa null-AR cells 10^{-8}M DHT.
Not Completed.

• With the lower priority placed on the importance of these studies, and with the necessity to follow-up other events more linked to the failure of prostate cancer treatment (Tasks 1, 2), these studies were jettisoned in favor of higher priority studies.

Other Progress

• We created a series of HeLa cell lines that expressed either CFP-AR-YFP or that expressed CFP-AR together with different amounts of AR-YFP. The cell lines, together with dramatic improvements in the level of automation of our FRET analysis, have enabled us to rapidly collect images from a large number of cells (see Fig. 9). This enabled us to rapidly complete our Tasks in the Statement of Work.

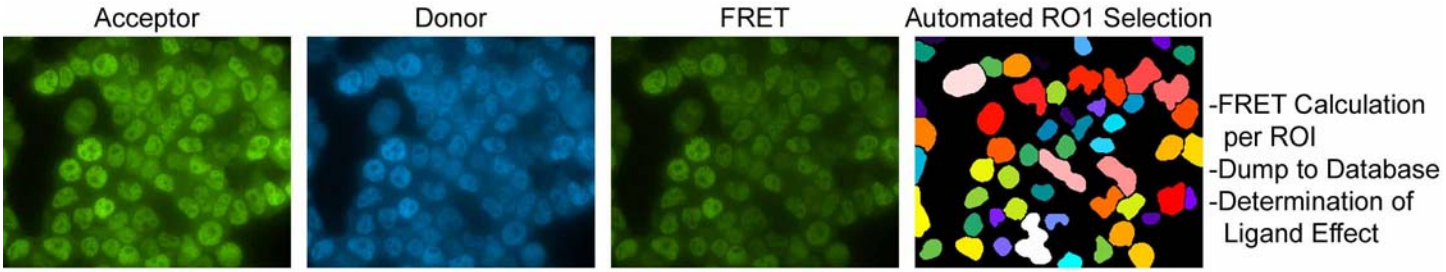

Fig. 9. Stable cell line expressing CFP-AR-YFP. Semi-automated image collection, followed by automated software recognition of cells and FRET calculation, have dramatically increased the speed by which we can collect data.

• Rapid data collection allowed us to pursue additional issues that are helping us to better understand the molecular events in AR associated with the generation of a hormone-resistant phenotype. We obtained a number of novel ligands from our collaborators (D.P. McDonnell, Duke University), who characterized their ability to activate transcriptional reporters and regulate the proliferation of LNCaP cells. We compared those activities against nuclear transport, CFP-AR/AR-YFP dimer FRET and CFP-AR-YFP FRET measured at UCSF (Table 1). We also examined those compounds for their response in our cell lines. This served both to confirm the appropriate activity of our fused AR in our cell lines and to establish that our cell lines faithfully were responding 'normally' to the added ligands. Note that the ability to promote transport of the AR into the cell nucleus correlates most strongly with LNCaP cell proliferation (yellow), which is the same conclusion reached in our comparisons of LNCaP and LNCaP-C4-2 cells (Task 2).

Table 1. Comparison of a panel of five ligands for their effects on transcriptional activity, prostate cell proliferation, AR nuclear transport, AR dimerization and AR folding.

Compound	Reporter activation (Duke)	LNCaP proliferation (Duke)	Nuclear transport (UCSF)	AR Dimer FRET (UCSF)	CFP-AR-YFP FRET (UCSF)	Reporter activation (UCSF)
no ligand	+	+	-	-	-	+
DHT	+++++	+++++	+++++	+++++	+++++	+++++
A	++	+++++++	++++	++	++	+++
B	+++	+++++++	+++++	+++++	+++	+++++
C	-	++	+	-	-	+
D	+++	+++++++	++	-	++	++
E	+++	+++++++	+++++	+++	++++	+++

• In what was intended as a negative control, our dimer FRET assays uncovered a ligand-regulated heterodimer of AR with the alpha isoform of the ER (not shown). It is possible that this AR/ER heterodimer may be important in anti-androgen therapy and the development of resistance to anti-androgen therapy. Due to the continued focus on achieving the original aims of the Statement of Work, this interesting finding was immediately followed-up but indicates an important point for future studies.

• By adding a 24 hour time point to our temporal analysis of FRET following DHT addition, we stumbled upon a 'maturation' even in which the AR assumes a different conformation (statistically significant FRET amount) 24 hours after the addition of ligand (see Fig. 4B). Some follow-up studies using the ΔF mutant showed that this maturation event did not occur if the FQNLF motif was deleted. Due to the continued focus on achieving the original aims of the Statement of Work, this interesting finding was not immediately followed-up.

• The folding of the FQNLF motif into the AF-2 pocket of the AR ligand binding domain would be expected to occlude that ligand binding domain. We established that the wild-type AR does not bind to the AF-2 interacting domains of three cofactors that interact with other nuclear receptors (although we observed those interactions with other receptors in an agonist ligand-dependent fashion). We also observed that deletion of the FQNLF motif, which would eliminate AF-2 blockade by this motif, did not permit the binding of those three 'SRC' cofactors. This suggested that, mechanistically, the known poor binding of the AR to these otherwise ubiquitously NR-interacting factors was not solely a consequence of FQNLF occlusion. This finding will likely be included as supporting data in a manuscript we are preparing of the interactions of these SRC cofactors with other NRs.

Key Research Accomplishments

1. Established that dihydrotestosterone addition to a live cell results in a very rapid, intramolecular folding of the AR, which is followed 3-5 minutes later by dimerization of the AR and by an even slower progressive transport of AR into the cell nucleus that takes place over the following hours.

2. Established methods for determining the effects of AR ligands or AR mutations on the interaction kinetics and structure of the AR dimer.

3. Established association of the anti-androgen actions of hydroxyflutamide and Casodex with a poor ability to promote nuclear transport, conformation and dimerization of wild-type AR.

4. Established correlation of AR nuclear transport, dimerization and intramolecular folding with four AR mutations associated with resistance to androgen deprivation therapy.

5. Established that the intramolecular fold within the AR required the FQNLF motif in the AR amino terminus and the AF-2 motif in the AR carboxy terminus. Dimerization is not dependent upon the FQNLF motif but the final conformation of the AR dimer is.

6. Established, using a novel panel of ligands that AR nuclear transport correlates best with LNCaP cell proliferation.

7. Established, by comparison of AR actions in androgen-dependent LNCaP cells with AR actions in androgen-independent LNCaP-C4-2 cells, that AR nuclear transport correlates best with androgen-independent cell proliferation.

8. Established image collection and analysis conditions for automated high throughput analysis of AR folding, dimerization and nuclear transport. Isolated and characterized cell lines that facilitate those studies. Together with the completion of our original Tasks which showed the relative association of AR folding, dimerization and nuclear transport with the establishment of treatment-unresponsive tumors, we are now prepared to screen large chemical libraries and siRNA libraries for factors that contribute to treatment-failure and novel drugs that counteract treatment failure. For this, a new automated high throughput screening system has recently been purchased for the laboratory.

Reportable Outcomes

1. One manuscript published (provided as an Appendix here)
Fred Schaufele, Xavier Carbonell, Martin Guerbadot, Sabine Borngraeber, Mark S. Chapman, Aye Aye K. Ma, Jeffrey N. Miner, and Marc I. Diamond. The structural basis of androgen receptor activation: Intramolecular and intermolecular amino–carboxy interactions. PNAS 2005 102: 9802-9807

2. One manuscript to be submitted soon describing the effects of the five novel ligands and bicalutamide, together with the previously published control hydroxyflutamide and dihydrotestosterone, on AR nuclear transport, dimerization and conformation in HeLa, LNCaP and LNCaP-C4-2 cells. The conclusions of those studies are detailed in this report.

3. One manuscript to be submitted soon describing the characterization and use of the CFP-AR-YFP and CFP-AR/AR-YFP cell lines in automated measurement of ligand-regulated intramolecular AR folding, AR dimerization and AR nuclear transport. The pitfalls of such measurements and the methods used to overcome those pitfalls will be detailed.

Conclusions

All Tasks in the Statement of Work were completed and even have been expanded by new technological innovations.

- Task 1 demonstrated a good correlation of enhanced nuclear transport, dimerization and intramolecular folding in response to anti-androgens and heterologous ligands of four different AR mutants isolated from patients with hormone-refractory prostate cancer.
- Task 2 demonstrated a correlation of enhanced, androgen-independent nuclear transport in an androgen-independent prostate cancer cell model (androgen-independent LNCaP-C4-2 cells compared to androgen-dependent LNCaP cells). Task 2 demonstrated no correlation of intramolecular folding of CFP-AR-YFP or dimerization of AR-CFP/AR-YFP with the acquisition of androgen-independence by the LNCaP-C4-2 cell line.
- Task 3 confirmed that the intramolecular fold between the amino and carboxy terminus in the AR depends upon the FQNLF motif in the AR amino terminus and AF-2 in the carboxy terminus.
- Other reportable outcomes from studies conducted under this grant funding, but not originally included in the Statement of Work, further demonstrated that the ability of different ligands to promoter cytoplasm-to-nuclear transport of AR best correlated with those ligands ability to regulate LNCaP cell proliferation.

References

1. Jemal A, Murray T, Samuels A, Ghafoor A, Ward E, Thun MJ 2003 Cancer statistics, 2003. CA Cancer J Clin 53:5-26
2. Geller J 1993 Basis for hormonal management of advanced prostate cancer. Cancer 71:S1039-S1045
3. Labrie F, Belanger A, Dupont A, Luu-The V, Simard J, Labrie C 1993 Science behind total androgen blockade: from gene to combination therapy. Clin Invest Med 16:475-492
4. Taplin ME, Bubley GJ, Shuster TD, Frantz ME, Spooner AE, Ogata GK, Keer HN, Balk SP 1995 Mutation of the androgen-receptor gene in metastatic androgen-independent prostate cancer. N Engl J Med 332:1393-1398
5. Wirth MP, Froschermaier SE 1997 The antiandrogen withdrawal syndrome. Urol Res 25:S67-S71
6. Laufer M, Sinibaldi VJ, Carducci MA, Eisenberger MA 1999 Rapid disease progression after the administration of bicalutamide in patients with metastatic prostate cancer. Urology 54:745
7. Joyce R, Fenton MA, Rode P, Constantine M, Gaynes L, Kolvenbag G, DeWolf W, Balk S, Taplin ME, Bubley GJ 1998 High dose bicalutamide for androgen independent prostate cancer: effect of prior hormonal therapy. J Urol 159:149-153
8. Taplin ME, Bubley GJ, Ko YJ, Small EJ, Upton M, Rajeshkumar B, Balk SP 1999 Selection for androgen receptor mutations in prostate cancers treated with androgen antagonist. Cancer Res 59:2511-2515
9. Taplin ME, Rajeshkumar B, Halabi S, Werner CP, Woda BA, Picus J, Stadler W, Hayes DF, Kantoff PW, Vogelzang NJ, Small EJ, 9663 CaLGBS 2003 Androgen receptor mutations in androgen-independent prostate cancer: Cancer and Leukemia Group B Study 9663. J Clin Oncol 21:2673-2678
10. Gregory CW, He B, Johnson RT, Ford OH, Mohler JL, French FS, Wilson EM 2001 A mechanism for androgen receptor-mediated prostate cancer recurrence after androgen deprivation therapy. Cancer Res 61:4315-4319
11. Gregory CW, Johnson RTJ, Mohler JL, French FS, Wilson EM 2001 Androgen receptor stabilization in recurrent prostate cancer is associated with hypersensitivity to low androgen. Cancer Res 61:2892-2898
12. Latil A, Bièche I, Vidaud D, Lidereau R, Berthon P, Cussenot O, Vidaud M 2001 Evaluation of androgen, estrogen (ER alpha and ER beta), and progesterone receptor expression in human prostate cancer by real-time quantitative reverse transcription-polymerase chain reaction assays. Cancer Res 61:1919-1926
13. Linja MJ, Savinainen KJ, Saramaki OR, Tammela TL, Vessella RL, Visakorpi T 2001 Amplification and overexpression of androgen receptor gene in hormone-refractory prostate cancer. Cancer Res 61:3550-3555
14. Culig Z, Hobisch A, Hittmair A, Peterziel H, Cato AC, Bartsch G, Klocker H 1998 Expression, structure, and function of androgen receptor in advanced prostatic carcinoma. Prostate 35:63-70
15. Wang LG, Liu XM, Kreis W, Budman DR 1999 Phosphorylation/dephosphorylation of androgen receptor as a determinant of androgen agonistic or antagonistic activity. Biochem Biophys Res Commun 259:21-28
16. Craft N, Shostak Y, Carey M, Sawyers CL 1999 A mechanism for hormone-independent prostate cancer through modulation of androgen receptor signaling by the HER-2/neu tyrosine kinase. Nat Med 5:280-285
17. Craft N, Sawyers CL 1999 Mechanistic concepts in androgen-dependence of prostate cancer. Cancer Metastasis Rev 17:421-427
18. Tyagi RK, Lavrovsky Y, Ahn SC, Song CS, Chatterjee B, Roy AK 2000 Dynamics of intracellular movement and nucleocytoplasmic recycling of the ligand-activated androgen receptor in living cells. Mol Endocrinol 14:1162-1174

19. Roy AK, Tyagi RK, Song CS, Lavrovsky Y, Ahn SC, Oh TS, Chatterjee B 2001 Androgen receptor: structural domains and functional dynamics after ligand-receptor interaction. Ann N Y Acad Sci 949:44-57
20. Fujimoto N, Mizokami A, Harada S, Matsumoto T 2001 Different expression of androgen receptor coactivators in human prostate. Urology 8:289-294
21. Mestayer C, Blanchere M, Jaubert F, Dufour B, Mowszowicz I 2003 Expression of androgen receptor coactivators in normal and cancer prostate tissues and cultured cell lines. Prostate 56:192-200
22. Scher HI, Kelly WK 1993 Flutamide withdrawal syndrome: its impact on clinical trials in hormone- refractory prostate cancer. J Clin Oncol 11:1566-1572
23. Schaufele F, Wang X, Liu X, Day RN 2003 Conformation of CCAAT/enhancer binding protein alpha dimers varies with intranuclear location in living cells. J Biol Chem 278:10578-10587
24. Weatherman RV, Chang C-Y, Clegg NJ, Carroll DC, Day RN, Baxter JD, McDonnell DP, Scanlan TS, Schaufele F 2002 Ligand-selective interactions of estrogen receptor detected in living cells by Fluorescence Resonance Energy Transfer. Mol Endocrinol 16:487-496
25. Day RN, Periasamy A, Schaufele F 2001 Fluorescence Resonance Energy Transfer Microscopy of Localized Protein Interactions in the Living Cell Nucleus. Methods 25:4-18
26. Day RN, Voss TC, Enwright III JF, Booker CF, Periasamy A, Schaufele F 2003 Imaging the localized protein interactions between Pit-1 and the CCAAT/enhancer binding protein alpha in the living pituitary cell nucleus. Mol Endocrinol 17:333-345
27. Ross SE, Radomska HS, Wu B, Zhang P, Winnay JN, Bajnok L, Wright WS, Schaufele F, Tenen DG, MacDougald OA 2004 Phosphorylation of C/EBP inhibits granulopoiesis. Mol Cell Biol 24:675-686
28. Schaufele F, Carbonell X, Guerbadot M, Borngraeber S, Chapman MS, Ma AA, Miner JN, Diamond MI 2005 The structural basis of androgen receptor activation: intramolecular and intermolecular amino-carboxy interactions. Proc Natl Acad Sci U S A 102:9802-9807
29. Saporita AJ, Ai J, Wang Z 2007 The Hsp90 inhibitor, 17-AAG, prevents the ligand-independent nuclear localization of androgen receptor in refractory prostate cancer cells. Prostate 67:509-520
30. Padron A, Li L, Kofoed EM, Schaufele F 2007 Ligand-selective interdomain conformations of estrogen receptor-alpha. Mol Endocrinol 21:49-61

Appendices

1. Current Contact Information:
Fred Schaufele
S-1230, 513 Parnassus
University of California San Francisco
San Francisco, CA, 94143-0540
Tel (415) 476-7086
FAX (415) 564-5813
email freds@diabetes.ucsf.edu

2. Published Manuscript:
Fred Schaufele, Xavier Carbonell, Martin Guerbadot, Sabine Borngraeber, Mark S. Chapman, Aye Aye K. Ma, Jeffrey N. Miner, and Marc I. Diamond. The structural basis of androgen receptor activation: Intramolecular and intermolecular amino–carboxy interactions. PNAS 2005 102: 9802-9807

The structural basis of androgen receptor activation: Intramolecular and intermolecular amino–carboxy interactions

Fred Schaufele*, Xavier Carbonell†, Martin Guerbadot*, Sabine Borngraeber‡, Mark S. Chapman§, Aye Aye K. Ma†, Jeffrey N. Miner§, and Marc I. Diamond†¶

*Diabetes Center and Department of Medicine, Departments of †Neurology, Cellular and Molecular Pharmacology, and ‡Biochemistry and Biophysics, University of California, San Francisco, CA 94143; and §Ligand Pharmaceuticals, San Diego, CA 92121

Edited by Keith R. Yamamoto, University of California, San Francisco, CA, and approved May 31, 2005 (received for review November 27, 2004)

Nuclear receptors (NRs) are ligand-regulated transcription factors important in human physiology and disease. In certain NRs, including the androgen receptor (AR), ligand binding to the carboxy-terminal domain (LBD) regulates transcriptional activation functions in the LBD and amino-terminal domain (NTD). The basis for NTD–LBD communication is unknown but may involve NTD–LBD interactions either within a single receptor or between different members of an AR dimer. Here, measurement of FRET between fluorophores attached to the NTD and LBD of the AR established that agonist binding initiated an intramolecular NTD–LBD interaction in the nucleus and cytoplasm. This intramolecular folding was followed by AR self-association, which occurred preferentially in the nucleus. Rapid, ligand-induced intramolecular folding and delayed association also were observed for estrogen receptor-α but not for peroxisome proliferator activated receptor-γ2. An antagonist ligand, hydroxyflutamide, blocked the NTD–LBD association within AR. NTD–LBD association also closely correlated with the transcriptional activation by heterologous ligands of AR mutants isolated from hormone-refractory prostate tumors. Intramolecular folding, but not AR–AR affinity, was disrupted by mutation of an α-helical (^{23}FQNLF^{27}) motif in the AR NTD previously described to interact with the AR LBD *in vitro*. This work establishes an intramolecular NTD–LBD conformational change as an initial component of ligand-regulated NR function.

conformation change | FQNLF | FRET | nuclear receptor | estrogen receptor

The nuclear receptor (NR) superfamily consists of a large group of ligand-regulated transcription factors. Several NRs are implicated in human physiology and disease (1, 2) and activation of the estrogen receptors (ER) and androgen receptors (AR) are predisposing factors for breast (3) and prostate cancer (4). Indeed, pharmacologic antagonists of AR and ER are used as antineoplastic agents in these diseases (4–7). It is commonly believed that understanding NR structure and function will facilitate development of specific drugs that can replace or supplement current therapies (2). Ligand binding alters NR structure, cofactor interactions, and transcriptional activity (8). Transcriptional activation functions are present in the amino-terminal domain (NTD; AF-1) and the ligand binding domain (LBD; AF-2) of many NRs, including AR (9) and ER (10). AF-1 is not conserved at the primary sequence level and is poorly characterized functionally (11). In contrast, AF-2 is highly conserved (12) and consists of amino acids that form a coactivator binding pocket on the surface of most NR LBDs (13–16).

In many NRs, both AF-1 and AF-2 activities are suppressed in the absence of ligand and enabled after ligand binding (9, 10), which implies that ligand binding to the LBD somehow unmasks AF-1 activities in the NTD. The molecular/structural basis for LBD communication with AF-1 in full-length molecules remains uncertain. However, an intermolecular interaction between NTD peptides and the agonist-bound LBD has been extensively characterized *in vitro* and with intracellular two-hybrid assays for the AR (14, 17–21) and ER (22). In the AR NTD, deletion or mutation of a sequence (^{23}FQNLF^{27}) that can bind the AF-2 coactivator pocket of the LBD (14, 19) diminishes activity of the AR at certain promoter elements (21). This finding suggests that an NTD–LBD interaction is functionally important, but it remains unknown whether the NTD interacts with the LBD within one molecule or whether it participates in an intermolecular interaction with the LBD of a second AR molecule.

Of the currently available experimental approaches, FRET (23) uniquely can resolve conformation changes and protein interactions of the intact NR molecule in living cells. FRET allows real-time detection of protein conformation changes based on energy transfer between fluorophores attached to domains of interest. Here, we used FRET to determine the time and subcellular location of ligand-induced conformational changes in AR that underlie its activity as a transcription factor. We contrasted these studies with other members of the NR family, ERα and peroxisome proliferator-activated receptor-γ2 (PPARγ2), and have determined a role for the AR-specific ^{23}FQNLF^{27} motif in coordinating intramolecular AR conformational changes that precede AR self-association, most likely as a dimer.

Materials and Methods

Plasmid Construction. Plasmids that express AR, ERα, or PPARγ2 as enhanced cyan fluorescent protein (ECFP)–NR, NR–enhanced yellow fluorescent protein (EYFP) or ECFP–NR–EYFP fusions were constructed by inserting PCR-amplified NR cDNAs into ECFP and EYFP-containing expression vectors (Clontech). The AR-AQNAA and ARΔF mutants were constructed by site-directed mutagenesis. AR LBD mutants were subcloned from full-length AR into CFP–AR–YFP. All constructs were sequenced after construction. The mouse mammary tumor virus (MMTV)-luciferase reporter plasmid was kindly provided by K. Yamamoto (University of California, San Francisco).

Cell Culture and Transfection. HeLa cells (n = 200,000) were split into each well of a six-well dish containing a borosilicate glass coverslip and grown in media containing newborn calf serum stripped of androgens. DNA (100 ng per well) was transfected by

This paper was submitted directly (Track II) to the PNAS office.

Freely available online through the PNAS open access option.

Abbreviations: AR, androgen receptor; CFP, cyan fluorescent protein; DHT, dihydrotestosterone; ER, estrogen receptor; FPR, fluorescence plate reader; LBD, carboxy-terminal domain; MMTV, mouse mammary tumor virus; NR, nuclear receptor; NTD, amino-terminal domain; OH-F, hydroxyflutamide; PPARγ2, peroxisome proliferator-activated receptor-γ2; YFP, yellow fluorescent protein.

¶To whom correspondence should be addressed at: University of California, GH-S572B, Box 2280, 600 16th Street, San Francisco, CA 94143-2280. E-mail: marcd@itsa.ucsf.edu.

www.pnas.org/cgi/doi/10.1073/pnas.0408819102

using Effectene (Qiagen, Valencia, CA). Cells were imaged live at the indicated time points (see Figs. 2–5 and Figs. 6–9, which are published as supporting information on the PNAS web site). HEK293 cells ($n = 1.5 \times 10^6$) grown in DMEM-H21 supplemented with 10% FCS were transfected in 3.5-cm dishes by using 1.2 μg of DNA with Lipofectamine Plus (Invitrogen). The day after transfection, 100,000 cells were replated to a 96-well dish in the presence or absence of hormone. Cells were fixed in 4% paraformaldehyde in PBS before reading on the fluorescence plate reader (FPR).

FRET Collection and Analysis. For FRET detection by microscopy, acceptor, donor, and FRET images were collected as described in refs. 24 and 25. For each cell, three fluorescence channels were collected: the acceptor channel (YFP excited with 496- to 505-nm light; YFP fluorescence collected at 520–550 nm); the donor channel (excited with 431- to 440-nm light; collected at 455–485 nm); and the FRET channel (excited with 431- to 440-nm light; collected at 520–550 nm). Cells separately expressing CFP–AR and AR–YFP established the individual contributions of the donor and acceptor fluorophores to each channel. Following the correction for the amount of background signal and for fluorescence contributed by the acceptor (YFP) to the FRET spectra, the level of FRET was established as the amount of FRET relative to donor fluorescence (FRET/donor). For tracking FRET over time, cells were maintained at 37°C during data collection using a stage warmer (Brooks Industries, Lake Villa, IL). Microscopy data were collected from cells expressing very low amounts of fluorescent protein-tagged AR. High-expressing cells were avoided. Comparing fluorescence values and amounts of a protein estimated by Western blot allowed us to roughly calibrate our equipment. We estimate that <50,000 AR–YFP were present in each of the >5,000 cells imaged in this study. Remarkably similar results were obtained by FPR, which relied on higher expression of AR for sufficient signal.

For FRET detection on the FPR (Safire, Tecan, Durham, NC), cells were cultured in black, clear-bottomed 96-well plates (Costar) as described in ref. 26, fixed, and read on the day of harvest. Measurements were taken from the bottom of the plate with the following settings: YFP, excitation at 485 nm/emission at 527 nm; CFP, excitation at 435 nm/emission at 485 nm; and FRET, excitation at 435 nm/emission at 527 nm. The excitation was performed ±2.5 nm, the emission was recorded ±6 nm. Each plate contained an untransfected cell control (background) and cells transfected with pure CFP and YFP expression plasmids (pECFP-C1 and pEYFP-C1; Clontech). Each data point was collected in quadruplicate. FRET/donor ratios were calculated after background subtraction and correction for acceptor (YFP) contribution into the FRET spectrum.

Luciferase Assays. HEK293 cells ($n = 1.5 \times 10^6$) were transfected in 3.5-cm dishes with a total 0.5 μg of MMTV-luciferase reporter and 0.05 μg of AR expression plasmid. Cells ($n = 100{,}000$) were subsequently replated in quadruplicate into a 96-well plate and cultured overnight with hormone. The following day, cells were washed and lysed. Lysate (5 μl) was read in 50 μl of 1× luciferase substrate mix (Pharmingen) on a luminometer (Ultra, Tecan).

Western Blots. HeLa cells transfected with the indicated expression vectors were grown with or without 100 nM dihydrotestosterone (DHT). After 24 h, whole-cell lysates or nuclear/cytoplasm extracts were prepared as described in ref. 24. Equivalent amounts of extract (15–20 μg) were resolved with SDS/PAGE and blotted with N-20 antibody (Santa Cruz Biotechnology) at 1:2,000. Bands were quantified with a digital imaging system (Alpha Innotech, San Leandro, CA).

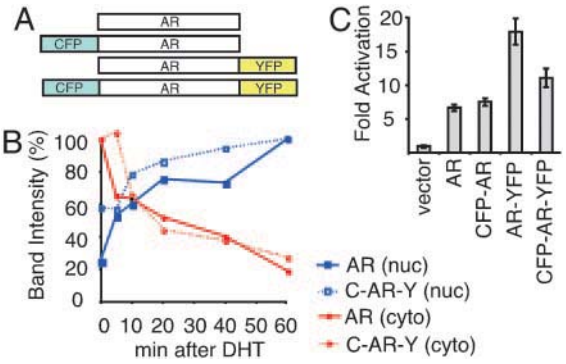

Fig. 1. AR-fluorescent protein fusions have normal responses to ligand. (*A*) Diagram of AR fusions to CFP and YFP. (*B*) An anti-AR antibody was used to probe nuclear (nuc) and cytoplasmic (cyto) extracts of HeLa cells expressing AR or CFP–AR–YFP (C-AR-Y) after treatment with DHT for different amounts of time. Quantification of band intensities (see Fig. 6*B* for blot) shows similar rates of ligand-induced nuclear transport for both. (*C*) MMTV-luciferase reporter activity increased when HEK293 cells expressing AR or AR fluorescent protein fusions were treated for 24 h with 100 nM DHT. The fold activity upon DHT addition is shown for each AR. Error bars represent the SEM.

Results

AR-Fluorescent Protein Fusions Preserve Basic Functional Activity. To investigate AR structure and function in the cellular environment, the AR was tagged with fluorescent proteins for expression in cells. The cDNA for CFP or YFP was fused to the amino and/or carboxy termini of AR to create CFP–AR, AR–YFP, and CFP–AR–YFP (Figs. 1*A* and 6*A*). The addition of the fluorescent proteins to both ends of the AR did not affect transport induced by the agonist ligand DHT. As expected (27, 28), AR and CFP–AR–YFP transiently expressed in HeLa cells were predominantly but not exclusively cytoplasmic in the absence of ligand and were transported into the nucleus upon DHT addition (Figs. 1*B* and 6*B*). Control blots with antibodies against tubulin or histone H1 demonstrated clean separation of the cytoplasmic and nuclear fractions (data not shown). Quantitative fluorescence imaging from multiple cells confirmed that CFP–AR–YFP and the singly fused CFP–AR and AR–YFP migrated at similar rates to the nuclei of HeLa cells after ligand addition (Fig. 6*C*). Finally, addition of DHT to HEK293 cells expressing the AR–YFP, CFP–AR, and CFP–AR–YFP fusion proteins activated reporter expression from a MMTV promoter similarly to that of unfused AR (Fig. 1*C*). Thus, basic function was preserved in all three AR fusion proteins, although the effects of CFP or YFP fusion on some other aspects of AR function can never be ruled out.

DHT Induces AR Self-Association Predominantly Within the Nucleus. AR dimerization is required for AR transcription activity (17). Therefore, AR dimers must be present in the cell nucleus, although it is unknown whether they form initially in the cytoplasm. We coexpressed CFP–AR and AR–YFP within HeLa cells and used quantitative FRET microscopy to determine whether the CFP and YFP were brought close enough (<80 Å) by AR interaction or association to allow efficient energy transfer. Transfer of energy from a donor fluorophore (CFP) to an acceptor fluorophore (YFP) results in decreased CFP (donor) fluorescence and increased YFP fluorescence upon CFP excitation (FRET). Thus, if energy is transferred from CFP–AR to AR–YFP, the FRET/donor fluorescence ratio (corrected for the contributions of the acceptor fluorophore to each fluorescence image; see *Materials and Methods*) increases relative to the FRET/donor fluorescence of CFP alone. Processed FRET/donor images from individual cells are shown in Fig. 2*A*. Image

CELL BIOLOGY

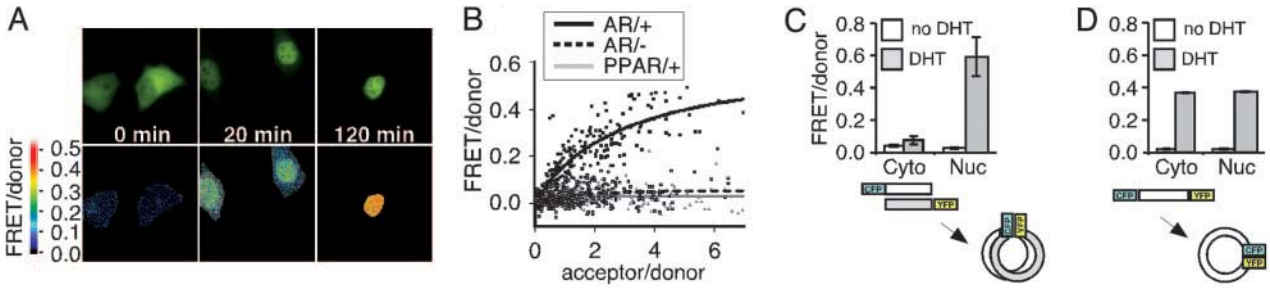

Fig. 2. AR dimerization and NTD-to-LBD folding measured by FRET microscopy. (*A*) HeLa cells expressing CFP–AR and AR–YFP were imaged at the indicated time points after addition of 100 nM DHT. (*Upper*) Acceptor signal. (*Lower*) FRET/donor images calculated from the corrected acceptor, donor, and FRET images (data not shown; see *Materials and Methods*). (*B*) Energy transfer of CFP–AR to AR–YFP (black boxes) increased with the relative amount of AR–YFP present to interact with CFP–AR (increasing acceptor/donor measured in the nuclei of 282 DHT-treated HeLa cells). There was no FRET in cells not incubated with DHT (open squares; 358 cells), nor was there FRET between CFP–PPARγ2 and PPARγ2–YFP in cells treated with the agonist ligand GW1929 (gray triangles; 215 cells). (*C*) Maximal, YFP-saturated FRET/donor values in the nucleus (Nuc) and cytoplasm (Cyto) of HeLa cells coexpressing CFP–AR and AR–YFP after treatment with 10 nM DHT or vehicle for 20 min. (*D*) FRET/donor values from cells expressing CFP–AR–YFP after treatment with vehicle ($n = 173$ cells) or 10 nM DHT for 20 min ($n = 80$ cells). Diagrams in *C* and *D* show the inferred changes in dimerization and conformation induced by DHT. Although the diagrams depict the amino and carboxy termini of the monomers in close proximity, our data allow no conclusion about the orientation of ARs within the dimer. Error bars represent the SEM.

processing introduces negative number errors, and the FRET data presented in all subsequent figures was more accurately calculated from large nuclear or cytoplasmic regions within the raw images.

Energy transfer was quantified in hundreds of CFP–AR- and AR–YFP-coexpressing cells. In nuclei of cells treated with DHT for 20 min, energy transfer from CFP to YFP increased with YFP amount until sufficient AR–YFP was present to saturate interaction with CFP–AR (Fig. 2*B*). The relationship of FRET amount to AR–YFP and CFP–AR amount fit well ($R^2 = 0.8$) to an equation (Fig. 2*B*, black line) that described an interaction between two molecules (24). For cells not treated with ligand (Fig. 2*B*, dotted line), there was no FRET, and the mathematical relationship suggesting a bimolecular interaction was not observed ($R^2 = 0.1$). Thus, in the absence of ligand, very few AR were detected in which the CFP and YFP were close enough (≈80 Å) to allow efficient energy transfer.

The amounts of FRET at saturating AR–YFP were determined in the nuclei and cytoplasm of cells treated with no ligand or with 10^{-8} M DHT for 20 min (Fig. 2*C*). DHT induced a strong increase in FRET that was significantly higher ($P < 0.01$) in the cell nucleus than in the cytoplasm. Similar analysis of intermolecular interaction was conducted with nuclear PPARγ2, which does not homodimerize (29). CFP–PPARγ2 and PPARγ2–YFP showed no association, even when incubated with ligand (Fig. 2*B*, gray line). Thus, a highly specific association of AR positions CFP and YFP close enough to permit FRET (<80 Å). Given the small distances involved, this FRET signal represents either direct dimerization between ARs or their simultaneous interaction with another factor that positions AR monomers not much more than a protein domain apart from each other. For simplicity, we shall refer to this self-association as "dimer FRET," particularly given the demonstrated bimolecular nature of the interaction.

Ligand Repositions the NTD and LBD Within AR. Conformational changes within AR monomers might precede dimerization. To investigate ligand-regulated structural changes within AR, we measured FRET between fluorophores attached to the same AR molecule (CFP–AR–YFP). In the absence of ligand, there was no significant FRET signal in the nucleus or cytoplasm of HeLa cells expressing CFP–AR–YFP (Fig. 2*D*). This finding indicated that the unliganded AR monomer was in an extended conformation and not self-associated. DHT induced CFP–AR–YFP FRET not only in the nucleus but also in the cytoplasm. Similar DHT-induced FRET in the cytoplasm and nuclei of CFP–AR–YFP-expressing cells (Fig. 2*D*) contrasted with lower dimer FRET in the cytoplasm (Fig. 2*C*), suggesting that portions of the DHT-induced cytoplasmic FRET from CFP–AR–YFP arose from an intramolecular event that brought the NTD and LBD into close proximity.

Intramolecular Folding of AR Precedes Association in the Nucleus. To establish whether intramolecular folding induced by DHT precedes or occurs simultaneously with dimerization in the nucleus, we measured the relative rates of ligand-induced folding and dimerization by using time-lapse studies of single cells. Intramolecular CFP–AR–YFP FRET and CFP–AR/AR–YFP dimer

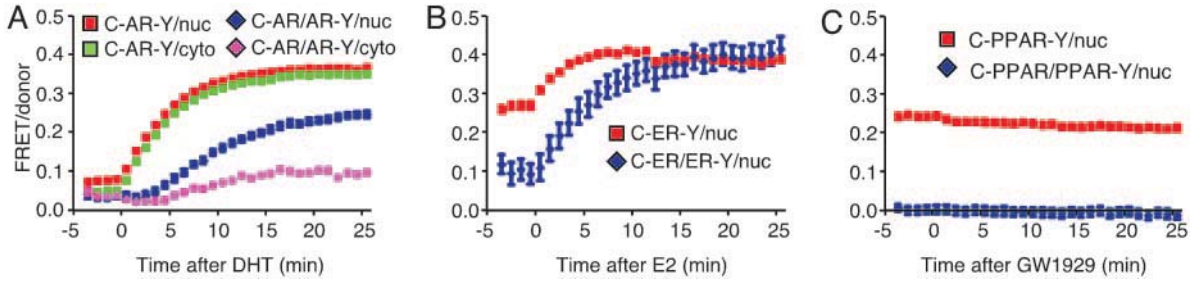

Fig. 3. Intramolecular folding precedes association of AR and ERα monomers but not PPARγ2. FRET was determined in HeLa cells expressing AR (*A*), ERα (*B*), or PPARγ2 (*C*) as fusions with CFP–NR and NR–YFP (association) or CFP–NR–YFP (folding). Images were collected every minute at 37°C. DHT (10 nM), estradiol (10 nM), or GW1929 (100 nM) was added 30 sec after the fourth image; an additional 26 images were captured starting 30 sec after the addition of ligand. The mean CFP–NR/NR–YFP or CFP–NR–YFP FRET in the nucleus (nuc; blue diamonds or red squares) and in the cytoplasm (cyto; pink diamonds or green squares) are shown from 12 or 47 cells (AR), 6 or 14 cells (ERα), and 8 or 11 cells (PPARγ2). Error bars represent the SEM.

FRET were measured within the cytoplasm and nucleus of HeLa cells at 1-min intervals before and after addition of 10 nM DHT (Fig. 3*A*). To ensure that dimer FRET and intramolecular FRET were detected with equivalent sensitivity, the dimer FRET studies were conducted with cells expressing high amounts of AR–YFP relative to CFP–AR (see Fig. 2*B*).

CFP–AR–YFP FRET increased rapidly after the addition of DHT, regardless of subcellular localization. The time required to reach half-maximal FRET ($t_{1/2}$) was ≈3.5 min in the nucleus and in the cytoplasm. The association kinetics of CFP–AR and AR–YFP (Fig. 3*A*) in the nucleus were significantly slower, with a $t_{1/2}$ of ≈9.5 min. We observed a similar, slower increase in FRET between CFP–AR-CFP and YFP-AR–YFP relative to CFP–AR–YFP in nucleus (Fig. 7) and cytoplasm. This finding ruled out the possibility that the fast accrual of CFP–AR–YFP FRET arose from a differential dimerization or transport kinetics of the dual-tagged AR in the nuclei of these cells. These results collectively imply that a rapid change in AR monomer structure precedes AR self-association.

Specificity of NTD–LBD Interactions Among NRs. To investigate whether ligand-induced rapid intramolecular folding was a common feature of NRs, we studied the intramolecular and dimerization kinetics for two other NRs. Unlike AR, ERα and PPARγ2 are predominantly nuclear in the absence of ligand. In the absence of estradiol, almost no ERα dimers were detected (Fig. 3*B*), just as nuclear-localized AR did not produce significant dimer FRET before ligand binding. However, unliganded CFP–ERα–YFP produced significant intramolecular FRET, indicating that, in contrast to AR, the fluorescent proteins attached to the NTD and LBD of unliganded ERα were closer than 80 Å. Upon estradiol addition, there was a rapid, further increase in intramolecular CFP–ERα–YFP FRET ($t_{1/2}$ ≈ 1.2 min) that significantly preceded the acquisition of dimer CFP–ERα/ERα–YFP FRET ($t_{1/2}$ ≈ 4.7 min). Thus, as with AR, ligand binding to ERα induced a rapid intramolecular fold and a slower dimerization. In contrast, PPARγ2, which biochemical evidence indicates does not form homodimers (29), showed no ligand-induced FRET from intramolecular folding or association (Fig. 3*C*), even though ligand addition caused CFP–PPARγ2- and PPARγ2–YFP-dependent activation of a PPAR-responsive reporter (data not shown). Thus, rapid intramolecular folding of the AR NTD and LBD followed by their close association within a presumed dimer pair is a feature shared with some but not all NRs.

NTD–LBD Folding Is Blocked by an AR Antagonist Ligand. To examine the functional significance of the NTD–LBD interactions, we tested the effects of a well characterized antagonist of AR transcription on intramolecular and dimer FRET. HEK293 cells were transfected with CFP–AR–YFP, plated in quadruplicate in a 96-well dish, and exposed to 10 nM DHT and increasing amounts of hydroxyflutamide (OH-F). After 24 h, cells were fixed and read on a FPR as described in ref. 26. The FPR rapidly measures thousands of cells and complements the more laborious microscopy-based technique. The strong FRET signal induced by DHT was competed effectively by excess OH-F in a dose-dependent manner (Fig. 4*A*). When measured by FRET microscopy, OH-F also inhibited CFP–AR–YFP FRET in the nuclear and cytoplasmic compartments of HeLa cells (Fig. 4*B*). Thus, OH-F binding prevents association of the NTD and LBD within a single molecule. OH-F also reduced cytoplasm-to-nucleus transport of CFP–AR–YFP (Fig. 8*A*) and did not promote FRET between AR–YFP and CFP–AR (Fig. 8*B*). Having observed that a transcriptional antagonist blocked intramolecular folding, we next examined the extent to which the FRET signal would predict AR transcriptional activity.

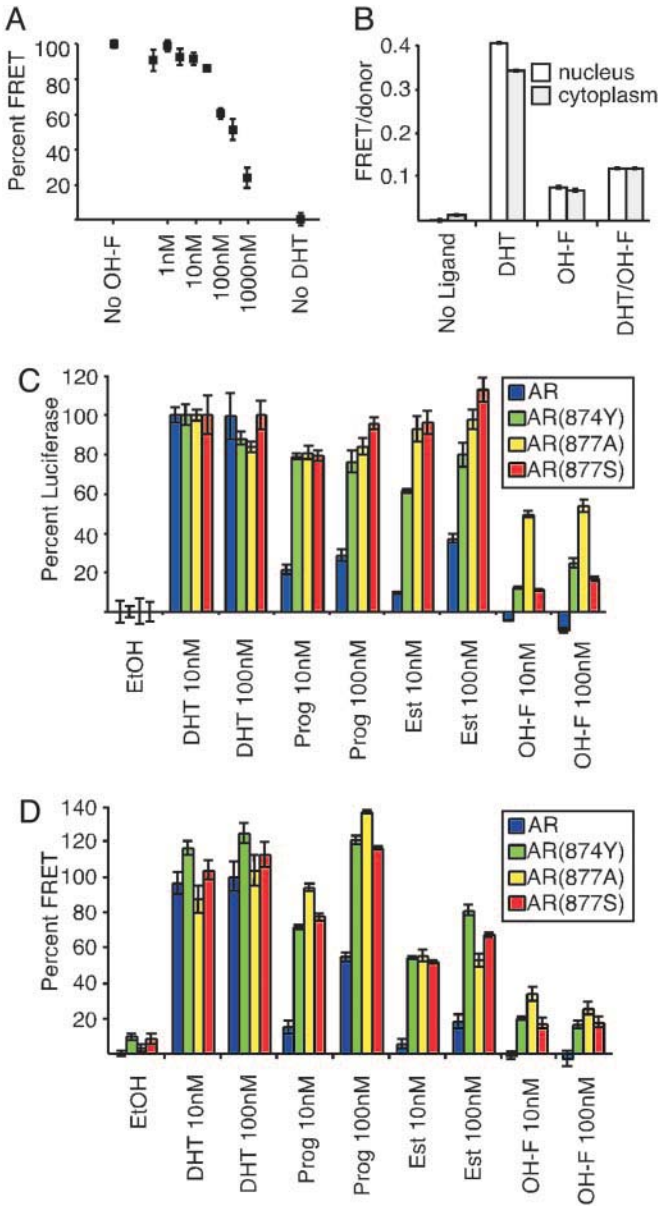

Fig. 4. AR NTD–LBD folding correlates with transcriptional activity. (*A* and *B*) OH-F antagonizes CFP–AR–YFP FRET in HEK293 cells treated with 10 nM DHT (detected by FPR) (*A*) and HeLa cells treated with 1 nM DHT with or without 1 μM OH-F (detected by microscopy) (*B*). (*C*) 847Y, 877A, and 877S AR mutants found in hormone-refractory prostate cancer allow progesterone (Prog), estradiol (Est), or OH-F to induce CFP–AR–YFP [and AR (32)] transcriptional activation of an MMTV-luciferase reporter in HEK293 cells. All mutants responded normally to DHT. Cells were cultured in quadruplicate in the presence or absence of the indicated ligands for 24 h. (*D*) FRET assays of the same mutants were performed after 24 h of culture in the presence of the indicated ligands. Error bars represent the SEM.

FRET Measurement of NTD–LBD Interaction Correlates with AR Transcriptional Activity. AR mutations have been isolated from hormone-refractory prostate tumors that permit AR transcriptional regulation in response to heterologous ligands, including OH-F, progesterone, and estrogen (30–33). Three of these AR mutants (H874Y, T877A, and T877S) were subcloned into CFP–AR–YFP and transiently expressed in HEK293 cells together with an MMTV-luciferase reporter. Transfected cells were cultured in the presence of 0, 10, or 100 nM DHT, progesterone, estrogen, or OH-F. As expected, wild-type CFP–AR–YFP responded

CELL BIOLOGY

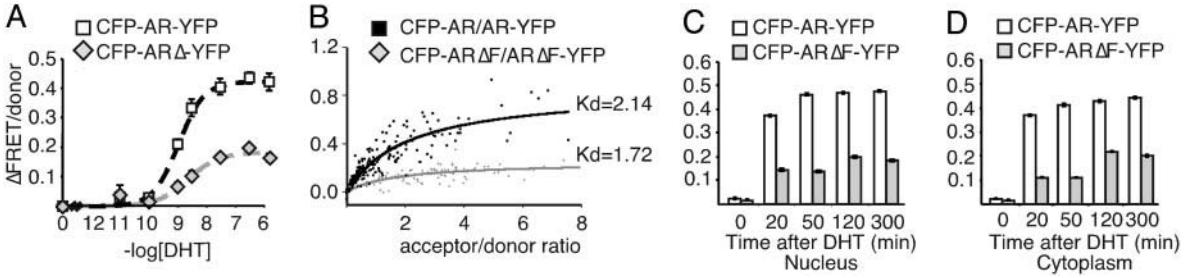

Fig. 5. The ^{23}FQNLF^{27} motif promotes NTD–LBD interactions within a single molecule. (*A*) Deletion of the ^{23}FQNLF^{27} motif had no effect on the DHT dose–response ($EC_{50} \approx 1$–3 nM) of CFP–AR–YFP FRET in HEK293 cells (detected by FPR). The overall level of CFP–ARΔ–YFP was lower than CFP–AR–YFP FRET. (*B*) Comparison of CFP–AR/AR–YFP and CFP–ARΔF/ARΔF–YFP association in HeLa cells. AR and ARΔF achieved maximum nuclear FRET at similar acceptor/donor ratios, indicating an equivalent dimerization affinity. Maximal FRET levels were reduced for the ΔF mutants, indicating an altered dimer structure. (*C* and *D*) HeLa cells transfected with CFP–AR–YFP ($n = 579$ total cells at all time points) or CFP–ARΔF–YFP ($n = 347$ total cells) were imaged by fluorescence microscopy within the nucleus (*C*) or cytoplasm (*D*) at various time points after addition of 100 nM DHT. Error bars represent the SEM.

strongly to DHT not only in the transcription assay (Fig. 4*C*) but also in the FPR-based FRET assay (Fig. 4*D*), whereas its responses to heterologous ligands were moderate (estrogen and progesterone) or minimal (OH-F). In contrast, the AR mutants induced parallel estrogen, progesterone, and OH-F activations of reporter gene activity and FRET. FRET microscopy studies in HeLa cells confirmed that these AR mutants partially restored AR NTD–LBD folding in the nucleus and in the cytoplasm (Fig. 9). The close parallel between the FRET-based biophysical readout (a direct measure of ligand-induced conformational change) and the reporter gene activation (an indirect measure of ligand-induced conformational change) suggested that the FRET signal reflected a transcriptionally competent AR conformation.

The ^{23}FQNLF^{27} Motif Orients the AR LBD and NTD Within Monomers. AR intramolecular folding may involve the previously described *in vitro* interaction between NTD and LBD fragments. That NTD–LBD interaction is mediated largely by the ^{23}FQNLF^{27} motif and other motifs in the AR NTD (20). However, it remains unclear whether ^{23}FQNLF^{27} participates in an intramolecular (folding) interaction or an intermolecular interaction.

We deleted the five amino acids comprising ^{23}FQNLF^{27} and tested the effect of this mutation (ARΔF) on AR structure. First, we used the FPR to compare the DHT dose–response for cells expressing CFP–AR–YFP or CFP–ARΔF–YFP. The EC_{50} of DHT for the induction of AR and ARΔF FRET was 1–3 nM (Fig. 5*A*). Introduction of alanine residues in place of phenylalanine and leucine (^{23}AQNAA^{27}) within the ^{23}FQNLF^{27} motif also reduced FRET in a manner similar to the ΔF mutation (Fig. 10, which is published as supporting information on the PNAS web site). Thus, disruption of ^{23}FQNLF^{27}did not impact the concentration of DHT required to achieve a steady-state conformational change in cells incubated for prolonged times with ligand.

The ^{23}FQNLF^{27} motif might participate in an NTD–LBD interaction between separate ARs to stabilize dimerization. We tested this possibility directly by measuring the intracellular association of AR and ARΔF using CFP–AR/AR–YFP FRET. No FRET was detected in the absence of DHT, but FRET was detected in DHT-treated cell nuclei for AR and ARΔF. Comparison of the donor/acceptor ratios to FRET indicated that both sets of data fit well with a curve that describes an interaction between two molecules (Fig. 5*B*), and the amounts of YFP-labeled AR required to achieve half-maximal FRET were statistically the same for the wild-type AR (2.14 ± 0.24, 95% CI) and ARΔF (1.72 ± 0.51), indicating similar self-affinities. Thus, deletion of the ^{23}FQNLF^{27} motif did not affect intracellular AR dimerization, and models of AR dimerization that assume a reliance on the interaction of FQNLF with AF-2 between monomers are not supported by our findings. However, the maximal FRET level was significantly higher for the wild-type AR than for ARΔF, which demonstrates that the FQNLF motif is required to properly orient the NTD and LBD domains between members of a dimer. We also found that deletion of ^{23}FQNLF^{27} reduced FRET from CFP–AR–YFP in the cytoplasm (Fig. 5*C*) and in the nucleus (Fig. 5*D*). Thus, the ^{23}FQNLF^{27} motif is required for maximal association of the NTD and LBD within AR and between AR molecules within a dimer but does not affect dimerization affinity.

Discussion

Live-cell FRET was used to precisely identify and characterize a ligand-induced NTD–LBD association within full-length AR. The agonist-induced conformation correlated well with transcriptional activity of the AR, in particular with those activities associated with acquisition of response to heterologous ligands in hormone-refractory prostate cancers (32, 34). The results are consistent with a model in which the unliganded AR exists in a relatively unfolded state in the cytoplasm and nucleus. After agonist binding, the AR rapidly converts to an active form in which the NTD and LBD within a single AR come into close association. The significant time periods (≈3.5 min) required for ligand-induced conformation changes may reflect the transit time of the ligand to the receptor or may suggest the involvement of other accessory factors in this process. In addition, the conformational change is followed ≈6 min later by AR association, which occurs more rapidly and efficiently in the nucleus. These findings imply that dimerization requires additional and compartment-specific molecular events.

Distinct NTD-LBD Interactions Among NRs. The NTD–LBD interactions of AR that follow ligand binding constitute one type of conformation change within the NR family. Estradiol also induced an NTD–LBD fold within CFP–ERα–YFP. In contrast, agonist had no effect on the interdomain structure of CFP–PPARγ2–YFP. Both ERα and PPARγ2 exhibited intramolecular FRET in the absence of ligand, whereas AR did not. It is possible that the higher baseline FRET levels of the unliganded ERα and PPARγ2 simply reflect the reduced distance between the NTD and LBD of ERα (595 aa) and PPARγ2 (505 aa) relative to AR (920 aa). Conversely, these different FRET levels might also represent distinct conformations specific to each unliganded NR.

It was recently reported that estradiol did not induce a conformational shift in CFP–ERα–YFP expressed in U2OS cells, whereas tamoxifen did (35). This study contrasts with our findings in HeLa cells and may indicate distinct ER structures or interactions under different cell environments and conditions.

For AR, which we studied in detail, FRET microscopy yielded similar results in HeLa and HEK293 cells. However, it remains to be determined whether analyses in other cell types might reveal distinct, cell-specific AR conformers.

^{23}FQNLF^{27}-Dependent and Independent NTD–LBD Associations. Prior work indicated that a NTD–LBD interaction in AR depended on the ^{23}FQNLF^{27} motif (14, 17–21). The data described here extends those studies by distinguishing between intramolecular and intermolecular events occurring within or between full-length AR molecules and by providing temporal and subcellular resolution of these processes. Prior *in vitro* studies suggested that the ^{23}FQNLF^{27} motif may not be the only contributor to NTD–LBD interaction (20). Indeed, we found that deletion of ^{23}FQNLF^{27} reduced but did not eliminate intramolecular FRET (Fig. 5), and it is likely that additional NTD–LBD interactions may aid or partially compensate the ^{23}FQNLF^{27}-dependent fold. Moreover, we observed a similar NTD–LBD fold for ERα, which does not contain an obvious FQNLF motif, supporting the idea that other NR domains can participate in ligand-activated folding. Because the ^{23}FQNLF^{27} motif is well described to interact with the coactivator binding pocket of the AR LBD (14), an intriguing possibility is that the rapid and relatively stable intramolecular fold prevents or modulates cofactor binding to the AR LBD, as has been recently suggested (14). This idea may help account for prior studies suggesting that, unique among the NRs, transcriptional activation by AR at certain promoters does not require cofactor binding to the LBD (9, 19). Given the association of this intramolecular fold with promiscuous responses in hormone-refractory AR LBD mutants, this intramolecular event may be a therapeutic target of considerable importance.

Conformation as a Measure of NR Activity. Traditional analysis of NR function has been based on biochemistry (e.g., ligand binding, DNA binding, cofactor binding), cell trafficking studies, and measures of transcriptional activity using reporter genes. Crystallographic studies of isolated NR LBDs have identified ligand-specific conformational changes in the LBD (13), but little is known of the structural basis of domain interactions within a full-length NR. An important new therapeutic strategy could be to target NR conformation through the allosteric modulation of domain interactions, distinct from competitive pharmacologic agents. Yet until now it has not been possible to directly measure NR conformational changes in the relatively physiologic context of an intact cell.

The FRET-based method described here offers opportunities to study the regulation of NR conformation in different cell types and possibly in different tissues of live animals. Combined with genetic manipulations in model organisms, FRET-band analyses may prove very useful for identifying cellular events that modify NR structure or protein interactions within the intracellular environment. Our finding that analysis of FRET via FPR faithfully reproduced many of the details uncovered by more laborious microscopic analyses suggests that FRET may provide a complementary, high-throughput method for detecting cellular or pharmacological events that specifically inhibit or enhance NR ligand-induced conformation change. This high-throughput capability may help identify drugs that operate differently in specific cell types or that induce alterations in the kinetics of conformation changes or protein interactions. Any or all of these approaches could have profound impact on understanding previously unrecognized pathways involved in NR action and may speed the discovery of new therapies for human diseases (2).

We thank Junlian Hu for expert technical assistance and Robin Chedester for assistance in manuscript preparation. This work was supported by U.S. Department of Defense Grants DAMD17-01-1-0190 and PC040777 (to F.S.), National Institutes of Health Grants R21 062782 (to F.S.) and R21 NS45350 (to M.I.D.), the Prostate Cancer Foundation (M.I.D.), Muscular Dystrophy Association Grant MDA3408 (to M.I.D.), and the Sandler Family Supporting Foundation (M.I.D.).

1. Katzenellenbogen, J. A., O'Malley, B. W. & Katzenellenbogen, B. S. (1996) *Mol. Endocrinol.* **10,** 119–131.
2. Gronemeyer, H., Gustafsson, J.-A. & Laudet, V. (2004) *Nat. Rev. Drug. Discovery* **3,** 950–964.
3. Chlebowski, R. T., Hendrix, S. L., Langer, R. D., Stefanick, M. L., Gass, M., Lane, D., Rodabough, R. J., Gilligan, M. A., Cyr, M. G., Thomson, C. A., *et al*. (2003) *J. Am. Med. Assoc.* **289,** 3243–3253.
4. Taplin, M. E. & Balk, S. P. (2004) *J. Cell Biochem.* **15,** 483–490.
5. Osborne, C. K. (1998) *N. Engl. J. Med.* **339,** 1609–1618.
6. Geller, J. (1993) *Cancer* **71,** S1039–S1045.
7. Baum, M., Budzar, A. U., Cuzick, J., Forbes, J., Houghton, J. H., Klijn, J. G., Sahmoud, T. & Group., A. T. (2002) *Lancet* **359,** 2131–2139.
8. McKenna, N. J. & O'Malley, B. W. (2002) *Cell* **108,** 465–474.
9. Simental, J. A., Sar, M., Lane, M. V., French, F. S. & Wilson, E. M. (1991) *J. Biol. Chem.* **266,** 510–518.
10. Metzger, D., Ali, S., Bornert, J. M. & Chambon, P. (1995) *J. Biol. Chem.* **270,** 9535–9542.
11. Kumar, R. & Thompson, E. B. (2003) *Mol. Endocrinol.* **17,** 1–10.
12. Danielian, P. S., White, R., Lees, J. A. & Parker, M. G. (1992) *EMBO J.* **11,** 1025–1033.
13. Feng, W., Ribeiro, R. C., Wagner, R. L., Nguyen, H., Apriletti, J. W., Fletterick, R. J., Baxter, J. D., Kushner, P. J. & West, B. L. (1998) *Science* **280,** 1747–1749.
14. He, B., Gampe, R. T., Kole, A. J., Hnat, A. T., Stanley, T. B., An, G., Stewart, E. L., Kalman, R. I., Minges, J. T. & Wilson, E. M. (2004) *Mol. Cell* **16,** 425–438.
15. Matias, P. M., Carrondo, M. A., Coelho, R., Thomaz, M., Zhao, X. Y., Wegg, A., Crusius, K., Egner, U. & Donner, P. (2002) *J. Med. Chem.* **45,** 1439–1446.
16. Sack, J. S., Kish, K. F., Wang, C., Attar, R. M., Kiefer, S. E., An, Y., Wu, G. Y., Scheffler, J. E., Salvati, M. E., Krystek, S. R. J., *et al*. (2001) *Proc. Natl. Acad. Sci. USA* **98,** 4904–4909.
17. Wong, C. I., Zhou, Z. X., Sar, M. & Wilson, E. M. (1993) *J. Biol. Chem.* **268,** 19004–19012.
18. Kemppainen, J. A., Langley, E., Wong, C. I., Bobseine, K., Kelce, W. R. & Wilson, E. M. (1999) *Mol. Endocrinol.* **13,** 440–454.
19. He, B., Kemppainen, J. A., Voegel, J. J., Gronemeyer, H. & Wilson, E. M. (1999) *J. Biol. Chem.* **274,** 37219–37225.
20. He, B., Kemppainen, J. A. & Wilson, E. M. (2000) *J. Biol. Chem.* **275,** 22986–22994.
21. He, B., Lee, L. W., Minges, J. T. & Wilson, E. M. (2002) *J. Biol. Chem.* **277,** 25631–25639.
22. Kraus, W. L., McInerney, E. M. & Katzenellenbogen, B. S. (1995) *Proc. Natl. Acad. Sci. USA* **92,** 12314–12318.
23. Zhang, J., Campbell, R. E., Ting, A. Y. & Tsien, R. Y. (2002) *Nat. Rev. Mol. Cell. Biol.* **3,** 906–918.
24. Schaufele, F., Wang, X., Liu, X. & Day, R. N. (2003) *J. Biol. Chem.* **278,** 10578–10587.
25. Weatherman, R. V., Chang, C.-Y., Clegg, N. J., Carroll, D. C., Day, R. N., Baxter, J. D., McDonnell, D. P., Scanlan, T. S. & Schaufele, F. (2002) *Mol. Endocrinol.* **16,** 487–496.
26. Pollitt, S. K., Pallos, J., Shao, J., Desai, U. A., Ma, A. A., Thompson, L. M., Marsh, J. L. & Diamond, M. I. (2003) *Neuron* **40,** 685–694.
27. Gregory, C. W., Johnson, R. T. J., Mohler, J. L., French, F. S. & Wilson, E. M. (2001) *Cancer Res.* **61,** 2892–2898.
28. Nightingale, J., Chaudhary, K. S., Abel, P. D., Stubbs, A. P., Romanska, H. M., Mitchell, S. E., Stamp, G. W. & Lalani, e.-N. (2003) *Neoplasia* **5,** 347–361.
29. Tontonoz, P., Graves, R. A., Budavari, A. I., Erdjument-Bromage, H., Lui, M., Hu, E., Tempst, P. & Spiegelman, B. M. (1994) *Nucl. Acids Res.* **22,** 5628–5634.
30. Veldscholte, J., Ris-Stalpers, C., Kuiper, G. G., Jenster, G., Berrevoets, C., Claassen, E., van Rooij, H. C., Trapman, J., Brinkmann, A. O. & Mulder, E. (1990) **173,** 534–540.
31. Taplin, M. E., Rajeshkumar, B., Halabi, S., Werner, C. P., Woda, B. A., Picus, J., Stadler, W., Hayes, D. F., Kantoff, P. W., Vogelzang, N. J., *et al*. (2003) *J. Clin. Oncol.* **21,** 2673–2678.
32. Taplin, M. E., Bubley, G. J., Shuster, T. D., Frantz, M. E., Spooner, A. E., Ogata, G. K., Keer, H. N. & Balk, S. P. (1995) *N. Engl. J. Med.* **332,** 1393–1398.
33. Gottlieb, B., Beitel, L. K., Wu, J. H. & Trifiro, M. (2004) *Hum. Mutat.* **23,** 527–533.
34. Fenton, M. A., Shuster, T. D., Fertig, A. M., Taplin, M. E., Kolvenbag, G., Bubley, G. J. & Balk, S. P. (1997) *Clin. Cancer Res.* **3,** 1383–1388.
35. Michalides, R., Griekspoor, A., Balkenende, A., Verwoerd, D., Janssen, L., Jalink, K., Floore, A., Velds, A., van't Veer, L. & Neefjes, J. (2004) *Cancer Cell* **5,** 597–605.